



HAL
open science

Vertical velocity field and convective plumes in the atmospheric boundary layer as observed with an acoustic Doppler Sodar

Odile Taconet, Alain Weill

► **To cite this version:**

Odile Taconet, Alain Weill. Vertical velocity field and convective plumes in the atmospheric boundary layer as observed with an acoustic Doppler Sodar. [Research Report] Centre de recherches en physique de l'environnement terrestre et planétaire (CRPE). 1981, 68 p., tableaux, graphiques. hal-02191853

HAL Id: hal-02191853

<https://hal-lara.archives-ouvertes.fr/hal-02191853>

Submitted on 23 Jul 2019

HAL is a multi-disciplinary open access archive for the deposit and dissemination of scientific research documents, whether they are published or not. The documents may come from teaching and research institutions in France or abroad, or from public or private research centers.

L'archive ouverte pluridisciplinaire **HAL**, est destinée au dépôt et à la diffusion de documents scientifiques de niveau recherche, publiés ou non, émanant des établissements d'enseignement et de recherche français ou étrangers, des laboratoires publics ou privés.

RP 182 (54)

B

**CENTRE NATIONAL D'ETUDES
DES TELECOMMUNICATIONS**

**CENTRE NATIONAL DE LA
RECHERCHE SCIENTIFIQUE**

**CENTRE DE
RECHERCHES
EN PHYSIQUE DE
L'ENVIRONNEMENT
TERRESTRE
ET PLANETAIRE**

CRPE

**NOTE TECHNIQUE
CRPE / 98**

*Vertical velocity field
and convective plumes in
the atmospheric boundary layer
as observed with
an acoustic Doppler Sodar*

120



Par
Odile TACONET
Alain WEILL

16 SEP. 1983

RESUME

Le champ de vitesse verticale dans la couche limite atmosphérique est observé à partir d'un sondeur acoustique Doppler. Cette étude présente deux points de vue :

1° le point de vue macroscopique :

relations entre la dissymétrie de la vitesse verticale et la vitesse convective, ainsi qu'un diagnostic de détermination des plumes convectives ;

2) le point de vue microscopique :

en utilisant les modèles de Telford 1970 et Manton 1975, une comparaison est effectuée entre la prédiction des modèles et les observations par Sodar. On met en évidence que les plumes transportent près de 60 % du flux de chaleur sensible disponible au sommet de la couche de surface.

**VERTICAL VELOCITY FIELD AND CONVECTIVE PLUMES IN THE ATMOSPHERIC
BOUNDARY LAYER AS OBSERVED WITH AN ACOUSTIC DOPPLER SODAR**

Odile TACONET and Alain WEILL
Centre National d'Etudes des Télécommunications,
Centre National de la Recherche Scientifique
C.R.P.E.
3 avenue de la République
92131 ISSY-LES-MOULINEAUX (FRANCE)

ABSTRACT

The vertical velocity field and the convective plumes are observed during the morning with the acoustic Doppler sounder of the C.R.P.E.. The study presents two points of view :

- 1) The macroscopic point of view : the histogram of vertical velocity in the well mixed layer associated with conditional averaging shows the relations between the vertical velocity skewness and the convective velocity w_* and gives an objective criterium for plume determination.
- 2) The microscopic point of view : using TELFORD's 1970 and MANTON's 1975 models, a comparison is made between the predictions of the models and the plumes properties as observed by the Doppler Sodar. It is shown that the convective plumes observed carry near sixty percent of the sensible heat flux at the top of the surface layer.

*C.R.P.E. (Centre de Recherches en Physique de l'Environnement)

**CENTRE DE RECHERCHES EN PHYSIQUE DE
L'ENVIRONNEMENT TERRESTRE ET PLANETAIRE**

NOTE TECHNIQUE CRPE/98

**VERTICAL VELOCITY FIELD AND CONVECTIVE PLUMES IN THE ATMOSPHERIC
BOUNDARY LAYER AS OBSERVED WITH AN ACOUSTIC DOPPLER SODAR**

par

Odile TACONET et Alain WEILL

RPE/BAP
Echelon Issy
3 Avenue de la République
92131 Issy-les-Moulineaux



Le Directeur Adjoint

I. REVAH

Le Responsable de l'Echelon

CRPE/Issy

P. BAUER

Mars 1981

**VERTICAL VELOCITY FIELD AND CONVECTIVE PLUMES IN THE ATMOSPHERIC
BOUNDARY LAYER AS OBSERVED WITH AN ACOUSTIC DOPPLER SODAR**

Odile TACONET and Alain WEILL
Centre National d'Etudes des Télécommunications,
Centre National de la Recherche Scientifique
C.R.P.E.
3 avenue de la République
92131 ISSY-LES-MOULINEAUX (FRANCE)

ABSTRACT

The vertical velocity field and the convective plumes are observed during the morning with the acoustic Doppler sounder of the C.R.P.E.. The study presents two points of view :

- 1) The macroscopic point of view : the histogram of vertical velocity in the well mixed layer associated with conditional averaging shows the relations between the vertical velocity skewness and the convective velocity w_* and gives an objective criterium for plume determination.
- 2) The microscopic point of view : using TELFORD's 1970 and MANTON's 1975 models, a comparison is made between the predictions of the models and the plumes properties as observed by the Doppler Sodar. It is shown that the convective plumes observed carry near sixty percent of the sensible heat flux at the top of the surface layer.

*C.R.P.E. (Centre de Recherches en Physique de l'Environnement)

**CENTRE DE RECHERCHES EN PHYSIQUE DE
L'ENVIRONNEMENT TERRESTRE ET PLANETAIRE**

NOTE TECHNIQUE CRPE/98

**VERTICAL VELOCITY FIELD AND CONVECTIVE PLUMES IN THE ATMOSPHERIC
BOUNDARY LAYER AS OBSERVED WITH AN ACOUSTIC DOPPLER SODAR**

par

Odile TACONET et Alain WEILL

RPE/BAP
Echelon Issy
3 Avenue de la République
92131 Issy-les-Moulineaux



Le Directeur Adjoint

I. REVAH

Le Responsable de l'Echelon

CRPE/Issy

P. BAUER

Mars 1981

1. INTRODUCTION

Convective activity and associated convective "structures" are of utmost importance if we want to know the mechanism of flux transfer from the ground surface up to the atmospheric boundary layer (A.B.L.). The knowledge of sensible heat flux as carried by thermal plumes is essential to understand, for modelling fast evolution of the A.B.L..

The purpose of this paper is to study the vertical velocity field associated with convective plumes as observed with an acoustic Doppler sodar and to consider, in connection with different theoretical models, what properties could be validated.

The meteorological situation investigated in this paper corresponds to clear air dry convective activity during morning solar heating, when the wind speed is smaller than ten ms^{-1} , in the mixed layer. The experiment takes place at VOVES near Chartres (in France) in July 1977 and in this study only the morning rise of the inversion layer detectable by the acoustic sounder till 10 L.T. is considered. The eulerian pattern of the convective field is associated with convective thermal cells, the typical horizontal scale of which is near 500 m up to one or two kilometers. Data evidence of such structures are reported by many investigators : KONRAD (1970), ROWLAND and ARNOLD (1975), NOONKESTER (1971), using a F.M.C.W. radar, KAIMAL et al. (1976) with a captive instrumented balloon, HALL et al. (1975) with an acoustic sounder.

In the literature, (considering experimental results) particular attention has been placed in two directions : first, the identification of these cells size and shape (eulerian and spatial). Second, the behaviour of the plume variables (mean temperature, humidity and velocity, vertical profiles and upward turbulent transfer). Early plumes measurements were performed by mean of an instrumented aircraft (WARNER and TELFORD, 1963, 1967). Above the Surface Layer (S.L.) (on a rough flat land or sea), TELFORD (1970) suggested a possible identification of plumes or thermals : "they are associated with patches and elevated fluctuating temperature relative to an uniform base temperature in the intervening regions, but turbulent intensity of velocity quite at the same level".

Recent campaigns were done with ground-based towers or balloons and aircraft (FRISH and BUSINGER (1973), KAIMAL (1976), PALMER and CAUGHEY (1978)) : FRISH and BUSINGER (1973) examine base-plume like temperature and vertical velocity structures in the Surface Layer (S.L.), by a statistical method ; they

found circular structures of small size (10 m) different from the plume tower size (500 m to several kms) in the mixed layer : (there should be a gap or a transition between the surface layer plume characteristics and the mixed layer). Considering velocity components spectra, generalized within the MONIN and OBUKHOV similarity, KAIMAL (1976) displays evidence of three dimensional turbulence of length scale $1.5 Z_I$. (Z_I is the height of the lowest inversion base). The vertical traces of temperature, heat and momentum flux provide also evidence of updraft of same scale, but no quantitative data of these inner variables are given, except in PALMER and CAUGHEY's work (1978), near $0.7 - 0.8 Z_I$.

Now, with remote sensing techniques as (Doppler radar and Doppler sodar), it has been possible to observe the mechanism associated with convective activity. In unstable situation, daytime sodar echoes above the surface layer are associated with plumes, the probable structure of the plumes was nearly vertical from HALL et al. observations (1975), with light winds (near 3 m/s). Recently, from SPIZZICHINO and VAN GRUNDERBEECK (1977), dimensions and locations of acoustic echoes and zones of updraft motion seem to be associated roughly with a vertical velocity normal distribution. Thus objective measurement of vertical velocity, in typical large convective cells is possible and their vertical profiles exhibit a maximum in the C.B.L., as for HALL et al. (1975).

The purpose of this study is to show that, from an eulerian field of convective cells depicted by sodar, each updraft can be isolated. Systematic measurements of some vertical profiles can be obtained (mean plume upward velocity, plume r.m.s. turbulent velocity) : their morning evolution, within the inversion rise detected by the sodar is investigated (between 7 h and 10 h L.T.) and, using a meteorological instrumented site, systematic data of the basic MONIN and OBUKHOV parameters are complemented.

Thus after a description of the data and the experimental features in part II, we shall present in a "macroscopic" point of view in part III the experimental vertical velocity distribution function as observed using acoustic sounder data : we shall consider properties of this statistical distribution, its validity and shall try to connect its main property (dissymetry) to the convective boundary layer parameters. Hence, in part IV we shall consider the "microscopic" point of view and relate the positive wing in the vertical velocity histograms to the plume structures, taking account of conclusions set up by MANTON (1975) and TELFORD (1970) models and finally we shall consider plume field properties in the well mixed layer : plume determination, plume vertical velocity parameterization, heat flux carried by elementary plumes, turbulent vertical velocity plume intensity, plume dimensions.

2. DATA AND EXPERIMENT FEATURES

The experiment took place in a flat corn field site in Beauce, located 100 km south east of Paris.

Acoustic reflectivity and vertical velocity were collected by the vertically pointed antenna of the three antenna Doppler sodar of CNET - CRPE. Main parameters of the sodar equipment used are given in (WEILL et al. 1980).

Examination of the facsimile record in the morning (8 h 30 - 9 h 00 T.L., July 6, 1977) (fig. 1) reveals features of updraft and downdraft motions capped by an inversion layer, connected with the mean micrometeorological characteristics of the boundary layer.

Basic similarity parameters of the A.B.L. are computed using :

a) Sodar measurement

- Mean wind and fluctuations profiles (mean horizontal velocity wind, Chong (1976)).
- A continuous monitoring of the inversion base Z_I (height of the maximum of reflectivity).
- Surface layer temperature flux Q_0 (using vertical velocity variance in dry convective situation) WEILL et al. (1980).
- Friction velocity U_* (KLAPISZ et WEILL, 1978).

b) Surface parameters measurement (by Institut National de la Recherche Agronomique I.N.R.A.)

- Surface heat flux measurement by a balance method of measurement for one hour using the B.E.A.R.N.* system (PERRIER et al., 1976).

*B.E.A.R.N. = Bilan d'Energie Albedo, Rayonnement Net

TABLE 1

MICROMETEOROLOGICAL CHARACTERISTICS

Date	\bar{U} Mean mixed-layer horizontal wind speed m/s	$d\bar{U}/dz$ in the well mixed layer	Z_1	Q_o surface heat flux W/m^2	U_* m/s	$-Z_1/L$ (till 10 h L.T.)
2 July morning 6 h 15 - 12 h 35		$\Delta\bar{U} = 4$ m/s for $\Delta Z = 220$ m	Strong morning	≈ 100	0,4	5
3 July 11 h 50 - 13 h 40	weak 3 to 4	≈ 0	inversion rise	≈ 40	0,25	bad estimates
6 July 6 h 40 - 16 h 40	6 up to 8.5	≈ 0		40	0,4	5
11 July 8 h 45 - 11 h	4.5 up to 6	≈ 0		≈ 100	0,4	10

- Friction velocity U_* and roughness length Z_0 from a 10 m instrumented tower.

c) Rawing-soundings by Etablissement d'Etudes et de Recherches Météorologiques E.E.R.M. (inversion height Z_I estimate from temperature profile).

d) Wind velocity, temperature, humidity from an instrumented aircraft (by E.E.R.M.).

The investigated convective mornings were (2, 3, 6, 11 July 1977) between 7 h and 11 h L.T., when the lower half of the C.B.L. was observed by the SODAR (cf. exemple table 1). Fig. 2 reveals the morning evolution of the basic parameters Z_I , Q_0 , U_* and Z_I/L (L is the MONIN-Obukhov length = $-\frac{U_*^3}{kg \frac{Q_0}{T}}$) the instability parameter of the Boundary Layer.

3. DISSYMMETRY OF THE VERTICAL VELOCITY DISTRIBUTION FUNCTION (The macroscopic point of view)

Sodar data are the vertical wind velocity W field, with a time resolution of 4 s and vertical resolution of 17 m, from the surface layer up to Z_I ($Z_I < 400$ m). Till now, few experimental vertical profiles of the third turbulent moment, W^3 , have been provided in the boundary layer (WEILL et al. 1978 ; FRANGI, 1978). An interesting problem is to connect this mean turbulent variable to the convective organization.

3.1 Characterization of $\overline{W^3}$ profile

The echosonde provides directly significant normalized profiles of $\overline{W^3}$ versus altitude (Z/Z_I) (WEILL et al., 1978). W^3 profiles collected at narrow instants gather together around a quasi parabolic mean curve (fig. 3) with a maximum around 0.3 - 0.4 Z_I and close to zero for 0.6 - 0.7 Z_I ; then W^3 increases below Z_I . Vertical velocity variance profiles W^2 are quite similar (ANDRE et al., 1978 - DEARDOFF, 1974 - WEILL et al., 1980).

Note the strictly positive value of $\overline{W^3}$, during the development of the morning convective activity (7 h to 12 h L.T.), except, when there is no effective convective organization as early July 2, 1977 (before 7 h 40) with a wind shear (4 m/s for a 200 m depth) (forced convection).

We observed $\overline{W'^3}$ maximum intensity increasing during solar heating : $\overline{W'^3}$ is normalized using $W_* = (Q_0 Z_1 / g T)^{1/3}$ (g gravity, T absolute temperature °K). Fig. 4 presents $\overline{W'^3}$ morning evolution during the four day experiments : vertical profile and maxima of normalized $\overline{W'^3}$ are bunching in a narrow range (the maximum of $\overline{W'^3} / W_*^3$ grows from 0.10 to 0.25) (cf. fig. 5), and $(\overline{W'^3} / W_*^3)$ is maximum in the C.B.L..

In fact, the averaging time used for $\overline{W'^3}$ will be chosen cautiously ; it depends on the length scale of vertical transfer, and we shall examine this point in the following paragraph.

3.2 Bimodal dissymmetry of the vertical velocity distribution function in convective situation

1° Bimodal dissymmetry characterization from a sodar velocity histogram

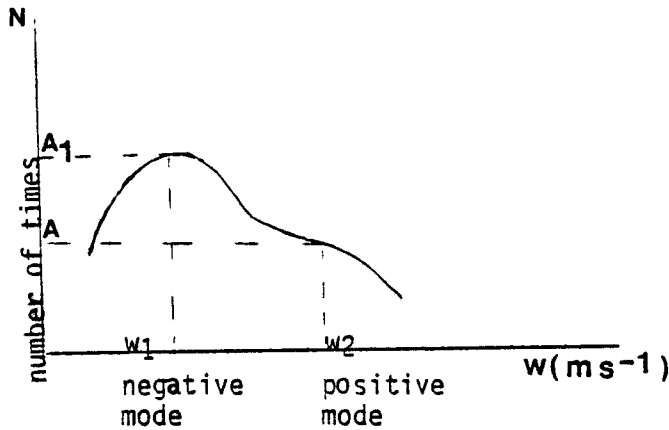
The vertical velocity distribution function is computed from data collected during a significant time, generally nearly half an hour and ordered in the 20 successive slices of histogram.

Histograms are shown cf. table 2 and fig. 6 (part 1 in moderately unstable situation, part 2 in unstable situation).

TABLE 2
HISTOGRAMS CHARACTERISTICS

Date	Convective conditions		Sodar period and hour	Z m	Z/Z ₁	Histogram velocity scale m/s	Slice width m/s	Total number of slices
	- Z ₁ /L	W _*						
6 July 1977	5	0.7	20 mn 8.51 → 9.11	73	0.3	- 1.8 → 2.0	0.19	20
2 July 1977	12	1.4	30 mn 10.45 → 11.15	243	0.2	- 1.8 → 3.0	0.24	20

The distribution function deviates from a normal one (with zero dissymmetry). The positive value $\overline{W^3}$ is associated with a different repartition of positive and negative velocities. There are more weak negative values than weak positive ones. Moreover, figure 6 (part 1) reveals, for strong positive value, (0.7 m/s) a large divergence from the normal curve, with a kind of wing (schema 1). The same feature exists on the other sample (fig. 6 - part 2). This hump appears as the secondary mode of a bimodal distribution, the first mode being associated with the main maximum of slightly negative values :



SCHEMA 1

This has to be justified. Therefore, first, we have to prove the generality of these results, and second, to study the relations of the two modes with mean characteristic features of parameters of the convective boundary layer.

2° Generality of these results

a) Data average period and conditional sampling

To be significant, the choice of the time duration T of velocity distribution function (that is the averaging period of turbulent momentum of $\overline{W^2}$ or $\overline{W^3}$) has to be associated with the increase in thermal plumes activity involving the capping inversion rise.

Rising inversions as observed by the CNET echosonde (fig. 7) reveals the juxtaposition of a secular rise (detected with a low pass filter of 20 mn) and oscillations of quite the same scales as the plumes (near 5 mn for 7 h 30 L.T.) : thus, the T eulerian time includes several temporal cross-sections of plumes.

Hence, during morning experiments, T changes and we use a conditional sampling based on the reflectivity facsimile examination and taking account of inversion height.

$$\text{In general, } T = \begin{cases} 20 \text{ mn from } 7.00 \rightarrow 9.00 \text{ L.T.} \\ 30 \text{ mn from } 9.00 \rightarrow 10.00 \text{ or } 11.00 \text{ L.T.} \end{cases}$$

and later we use 40 mn or 60 mn depending of cell sizes.

This choice is valid for the convective layer ($0.2 < \frac{Z}{Z_I} < 0.7$), but not above, where entrainment processes occur on different scales : this is revealed by the deviation of the averaged vertical velocity $\overline{W}_T(Z)$ from zero, especially above $0.7 Z_I$ and below $0.2 Z_I$ (fig. 8).

b) Histogram resolution

Two requirements are met.

- First, the histogram slice width must be large enough to include the random measurement inaccuracies : (these are mainly due to the random nature of the backscattered sodar signal and atmospheric turbulent inhomogeneities (Spizzichino, 1974), and amount to $|\Delta W| < 0.2 \text{ m/s}$). The chosen histogram resolution is of the same order of magnitude (0.2 m/s and 0.25 m/s). To simplify the comparison between different histograms, only 20 slice histograms are used with two total velocity length scales (-1.8 m/s \rightarrow 2.0 m/s and -1.8 m/s \rightarrow 3.0 m/s) and respectively a resolution of 0.12 m/s and 0.25 m/s). A lack of precision is added by aberrant data at higher altitude than (200 m), top of the plumes, where the echoes are very weak (Fig. 9).

- Second, histogram slices must be narrow enough to locate the positive velocity wings, more difficult to determine than the main weakly negative mode, characterized without ambiguity. To detect the existence of the hump, it must be located, at least, on a quarter of the histogram. For example, the July 2 histogram (fig. 6 - part 3) reveals a wing width of around 0.9 m/s for a total velocity scale of 3.8 m/s.

c) Increase of the degree of generality - Averaged histogram on several altitudes

Just above, two data procedures were presented to justify the chosen characteristics and analysis of histograms and provide bimodal distribution evidence.

Furthermore, this characterization is strengthened by the comparison of quasi-independent samples (histograms), taken during the same period of time, but at successive vertical sodar gates (separated by 17 m) across the C.B.L. (up to $0.7 Z_1$). Eight to fifteen gates can be studied in early morning when Z_1 is smaller than four hundred meters.

Independently of their variability, each reveals a bimodal repartition (fig. 10). Thus, for a same time period, independent values of the two velocity modes (W_1, W_2) and intensities (A_1, A_2) are estimated (schema 1).

The negative mode velocity, W_1 , is really associated with the negative main maximum and the second mode velocity, W_2 , to the middle of the wing.

From one sample, the determination of W_2 is unaccurate (in a range of two histogram slices, i.e. of about ± 0.20 m/s), but juxtaposition of independent histograms increases W_2 significance. The Students't distribution is then used to test the coherence of the two modes estimates within a 15 % precision (it is a severe normality test for limited population (here < 15 samples)). At least half of the tested population is within the confidence interval and corresponds generally to the well mixed layer.

First, we have studied the generality of bimodal dissymmetry. Second, we shall now study the connection between the 2 modes and characteristics features of the C.B.L.. Hence, at first we have to consider the morning evolution of vertical velocity histograms, showing the relation with C.B.L. evolution, using sodar samples or independent aircraft measurement. Then, we shall be able to parameterize the different modes using the A.B.L. parameters.

3° Dissymmetry evolution during the convective development of the boundary layer

a) Sodar samples

The examination of height averaged histograms in moderate and fully developed convection of different mornings proves the generality of the bimodal behaviour of the vertical velocity distribution (fig. 11). Bimodal feature is more pronounced in developed convective situations.

b) Other validation - Aircraft samples

Comparison between aircraft and our echosonde variance estimates have been made by WEILL, GOUTORBE and VAN GRUNDERBEECK (1978). From their work, discrepancies between spatial (aircraft) and eulerian (echosonde) measurements seem caused by the importance of low frequencies in the case of aircraft estimates. To eliminate low frequencies contribution, the aircraft run was reduced (flights of 5 km along the wind for our studied cases). Notice that an echosonde averaging period of 30 mn (often used in our samples) corresponds to the same order of magnitude as the aircraft flights (5 to 10 km long), using Taylor's hypothesis with light wind speed of 3 to 6 m/s.

Furthermore, the eulerian and spatial approaches could be compared in a quasi-stationary and homogeneous situation. Such a case appears here, at 11 L.T., in fully developed convection, but the inversion is high ($Z_1 > 1$ km) and only 1/3 of the C.B.L. is observed by the echosonde.

Only four histograms could be compared after 11 h (same altitude and instant as sodar ones) (fig. 12).

The variance discrepancies are small (the sodar vertical velocities are lower than aircraft ones by around 15 % : same results as WEILL, GOUTORBE and VAN GRUNDERBEECK (1978).

The main maxima in the sodar histograms are nearly zero, but the aircraft ones are slightly negative, may-be because of a skewness in the calibration of vertical velocity between the two instruments : (the differences between the two estimates of W_1 and W_2 are at the very most of 40 %). This observation can be considered as a redondant proof of bimodal vertical velocity histogram signature.

3.3 Normalization of the two modes velocities by velocity scaling W_*

The two modes are representatives of the convective organized structure (updraft and downdraft), and it seems interesting to parameterize them using W_* .

The positive mode intensity increases while the convective activity strengthens the wing. Its normalized variation by W_* is linear, (first approximation) (fig. 13). A rate of increase of the two modes intensities is proposed :

$$\begin{cases} W_1 = -0.3 W_* + 0.05 & \text{within a scattering of } \pm 25 \%, \\ W_2 = +0.5 W_* + 0.17 \end{cases}$$

but other measurements in late morning and greater unstable conditions ($-Z_T/L > 10$) must be pursued.

Considering the inaccuracies of the 2 modes (within $\pm 20 \%$) caused by their method of determination and imprecision, considering also the good agreement between sodar and aircraft estimates ($\pm 20 \%$), and the incertitude on W_* (15 %), a scattering of 25 % around the linear variation is satisfactory.

Now we shall present the second aspect of our dichotomic analysis and propose an objective threshold velocity for positive plume velocities since W_2 is correlated to the convective activity and normalized within the framework of W_* scaling. This velocity, strongly positive, gives obviously an order of magnitude of the thermal velocity.

The velocity connected with the beginning of the histogram positive wing (within ± 0.2 m/s) could be considered as a threshold for velocity belonging to upward motion (plumes) ; this threshold seems to be a more accurate and significant test than a threshold velocity simply equal to zero as in MANTON (1977) (cf. fig. 14). That will be the subject of this part of our study, the microscopic point of view : thermal cells critical modelling analysis and experimental validation.

4. THERMAL CELLS MODELLING AND TURBULENT STRUCTURE OF CONVECTIVE CELLS INVESTIGATED WITH AN ACOUSTIC DOPPLER SOUNDER : (the microscopic point of view)

The dissymmetry signature $\overline{W'^3}$ of the random field of turbulent velocity W is connected with a bimodal distribution and has been normalized by W_* in morning convective situations. This behaviour seems to justify model of the organized convection by two discrete entities (plumes or thermals and the surrounding

A starting point is the comparison of two organized convection models (TELFORD (1970) and MANTON (1975)), above the surface shear layer : they give theoretical predictions and hypothesis, interesting to study or to confirm using sodar observations.

4.1 TELFORD (1970), MANTON (1975) modelling : a comparison

Notice the similar and complementar arrangement of assumptions and constraints of the two models.

- TELFORD models a thin morning boundary layer ($Z_1 \simeq 400$ m) interacting with a very stable capping inversion ; the heat flux is transferred by a field of continuous plumes.

- MANTON presents a model of field of thermals : the depth of the layer is near 1-2 km, (height of the synoptic inversion layer Z_1) and Z_1 does not affect thermal mechanics.

Hence the updraft nature and entrainment processes are different but always in clear air.

Updraft and downdraft are considered individually, with distinct mean variables, then hypotheses on the turbulent nature of these cells and the constraints caused by neighbouring motions are formulated, together with boundary conditions, expressing the vertical structure of the C.B.L..

The treatment of turbulent interactions is different : for TELFORD, only an updraft and its surrounding downdraft will be examined neglecting the influence of the other updrafts (but one thermal cell modelling) : turbulent air interchange between the two drafts is great and normalized within the scaling of the r.m.s. turbulent velocity of each entity. In MANTON, the two kinds of interactions between 2 cells, (between updraft motion and descending air) is accounted for implicitly by imposing the original and simple condition that f (fraction of area occupied by convective elements) is constant with height : field of thermal cells modelling.

In MANTON's work, no turbulent dissipation, no Z_1 influence and no change of the mean air density because of heating are taken into account.

Table 3 summarizes the theoretical results and point to be confirmed using acoustic sounder data.

TELFORD (1970) ,MANTON (1975) MODELS : A COMPARISON

PROPERTIES STUDIED IN THE TWO MODELS	TELFORD (1970)	MANTON (1975)	POINT TO BE CONFRONTED WITH SODAR OBSERVATIONS
Micrometeorological situation	Thin morning convective boundary layer ($Z_1 < 400$ m)	Synoptic boundary layer (Z_1 , 1 to 2 km) late morning	
Influence of inversion layer	It is a very stable one with no entrainment processes	No influence on thermal mechanics	
Observed convective field	Field of continuous plumes	Field of discrete thermals	Study of the eulerian field
Influence of neighbouring cells (cell = updraft + surrounding downdraft)	No constraint between 2 cells	Lateral spread of thermal is constrained by the neighbouring cells (condition on f : $f = \frac{S_{updraft}}{Total\ surface} = 1/2$)	
Vertical velocity distribution function in each entity	Uniform	Uniform	
Lateral mixing between updraft and downdraft	Entrainment velocity is proportional to the r.m.s. turbulent velocity of the mixing region	Connected to thermal acceleration	
Updraft shape and size	Circular plume, horizontal size constant up to $0.7 Z_1$ and increases up to Z_1	Random shape, thermal volume increases up to $0.6 Z_1$, then constant	Study of the eulerian field
Determining parameters for cell size	Qualitative analysis of surface heat flux and Z_1 influence	No parameter	
Fraction of area occupied by convective updraft	Order of magnitude: $f \approx 0.3$, but depends on Z_1 and surface heat flux	Imposed value: $f = \text{constant}$ with height = 1/2	

TABLE 3 part1

PROPERTIES STUDIED IN THE TWO MODELS	TELFORD (1970)	MANTON (1975)	POINTS TO BE CONFRONTED WITH SODAR OBSERVATIONS
Boundary conditions at Z_T	1) temperature excess (updraft and downdraft) zero at Z_T 2) turbulence intensity is the same in updraft and downdraft 3) upward velocity is not zero	No conditions	
Boundary conditions at the top of the surface layer	Turbulence intensity is the same in updraft and downdraft	Initial temperature excess and velocity of thermals are determining	
VERTICAL PROFILES			
Upward velocity profile $W_p(Z)$	Maximum near $0.5 Z_T$	Increases up to $0.6 Z_T$ then constant	Vertical profile of $W_p(Z)$
Downward velocity profile $W_e(Z)$	Telford gives the profile of $(W_p - W_e)(Z)$		
Ratio between W_p and W_e	As the ratio of respective surfaces	As the ratio of respective surfaces	
Profiles of the r.m.s. turbulent velocity of each entity (i_p and i_e)	i_p and i_e are quasi constant with height in a ratio $\frac{i_p}{i_e} = 1$	No prediction of this variable	Measurements of i_p and i_e
Profile of the temperature excess between updraft and downdraft	It decreases linearly and is zero at Z_T (no heat flux transfer across the inversion)	It decreases and becomes zero at $0.6 Z_T$	
Turbulent heat flux carried by upward motions	Plumes would transfer only around 70 % of the surface heat flux, $\frac{Q_{plume}}{Q_{total}} = 1 - f_{plume}$	Thermals carry only around 30 % of the surface heat flux, $\frac{Q_{thermal}}{Q_{total}} = 1 - f_{thermal}$	Estimations of heat flux carried by plumes
Thus: $\frac{Q_{plume}}{Q_{total}} = 1 - \frac{S_{plume}}{S_{total}}$ (cf Appendix I for this computation)	Telford and Manton consider only the average potential heat flux on a convective cell as a whole (updraft + downdraft), but it seems interesting to <u>separate the heat flux contribution of each motion</u> . We compute it by using variables and equations of Telford model.		

TABLE 3 part 2

4.2 Experimental determination of the eulerian field of plumes in the mixed layer

Facsimile record of backscattered acoustic intensity and Doppler velocity reveals continuous plumes from the top of surface layer to Z_1 .

According to HALL et al. (1975), the location of the plume edges, from "Reflectivity" facsimile, is somewhat ill-defined: within plume boundaries, there are localized regions of much greater temperature structure, or "plumes within plumes".

In WARNER and TELFORD (1963), the structures are less clearly identified from the velocity patterns than from the temperature ones, since the character of the fluctuating vertical velocity is not markedly different in the updraft and downdraft.

Thus, tests of plume determinations should be cautiously specified from sodar data (reflectivity and Doppler velocity), they are first defined from only one examination of the turbulent vertical velocity field.

1° Determination tests from velocity field examination

a) In paragraph IV-3, an objective threshold velocity for positive plume velocities was proposed (velocity connected with the positive wing in the histogram, within ± 0.2 m/s).

This test is objective: it is evidence of the bimodal signature of the velocity field, and hence to the separation of convective transfer between two entities.

This test is evolutive: bimodal dissymmetry increases with the development of convective activity (cf. paragraph 3-3). The selected record corresponds to one hour and assuming that it does not change the threshold velocity, W_{th} is deduced from histograms averaged through the convective layer (from $0.2 Z_1$ up to $0.8 Z_1$), but during averaging period of 20 or 30 mn. No significant difference of W_{th} estimate is found by evaluating the W_2 variations on 1 hour (same magnitude as W_{th} variations), and using normalized relation between W_2 and W_* . The results are summarized in table 4: variations are inferior to 0.07 m/s, clearly within the precision of one histogram slice.

TABLE 4

W₁ AND W₂ VARIATION DURING ONE HOUR

Date	Hour	$\Delta w_{1m/s}$	$\Delta w_{2m/s}$	$\frac{\Delta w_2}{w_2}$
July 6	7 h - 8 h	0.20	0.07	40 %
	8 h - 9 h	0.05	0.02	8 %
	9 h - 10 h	0.10	0.05	14 %
July 11	8 h 10 - 9 h 10	0.07	0.03	8 %

TABLE 5

Date	Hour	W _{th} Threshold m/s
July 6	7.50 - 8.10	0.3
	8.51 - 9.11	0.4
	9.37 - 10.07	0.4
July	8.10 - 8.30	0.4

Computed threshold velocities for selected samples are summarized in table 5.

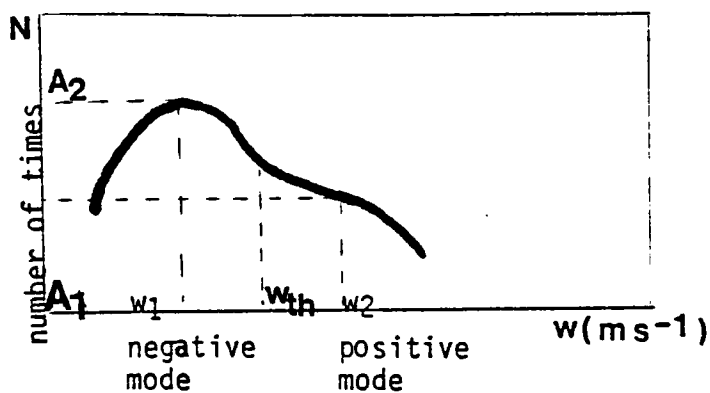
Above $0.8 Z_p$, no velocity test is determined. Plume velocities are weak and entrainment processes occur.

b) As observed by Hall et al. (1975), the structure inside the plume is not uniform, but small downward eddies must be taken into account.

A maximum temporal eddy size inside plume (t_1) is specified from computation of the separation time between base family plumes located from reflectivity facsimile and also from coherence of vertical plume boundaries at successive sodar gates : $t_1 = 30$ s (seven times sodar repetition rate of 4 s) for an usual plume duration of 2 up to 5 mn. Hence, from this second test, updrafts lasting less than 30 s are not considered.

These 2 tests are sufficient to locate individual plumes from only velocity field data (cf. fig. 15).

Then a question is raised : could the threshold velocity test be too drastic to locate plume edges ? A plume would not be rejected, if it has sharp boundaries, i.e. if there is a strong horizontal gradient of vertical velocity, at the edges of the plume. This hypothesis is confronted to observations, by determining plume boundaries using the two tests, t_1 and W_{th} , but with various values of the threshold velocity (0.2 m/s to 0.6 m/s).



SCHEMA 2

On this schema, the determined boundary does not change with W_{th} variation between 0.2 m/s and 0.4 m/s, and the acceleration is at least 0.2 m/s in 4 s.

For the tested plume (cf. fig. 16, plume 5 of July 11 around 8.30), for example, the upwind edge, occurring later in time, is sharp. The threshold velocity varies from 0.2 to 0.6 m/s, and the boundary of 0 to 6 sodar shots (0 to 24 s). Notice that, in the moderate convection of the mornings studied, the mean upward velocity in the plume is usually of magnitude < 1 m/s ; thus a jump of 0.4 m/s in few seconds is considered as an abrupt transition. Remark that six sodar shots for five minutes plume duration correspond to only 8 % of the plume surface.

All plumes of the sodar field were tested (width between 0.2 and 0.6 m/s). 50 % of them have clearly sharp boundaries, and they represent the most energetic of the field, so the most important for convective activity. Other plumes have a weak velocity short duration and often don't reach the inversion layer.

2° Correlation between "acoustic reflectivity" and vertical Doppler shift

As presented by ARNOLD et ROWLAND (1975), SPIZZICHINO and VAN GRUNDERBEECK (1977), the location of acoustic echoes and the base of the zones of upward motion are found to correspond.

So, the location of base plume edge can be confirmed by direct confrontation with acoustic "reflectivity", but with no significant additional precision.

4.3 Vertical profile of plume velocity and elementary sensible heat flux carried by each plume

Velocity profiles in plumes, versus normalized height Z/Z_I , display a systematic maximum near 0.3 - 0.4 Z_I (fig. 17). This maximum, not normalized, was found in some profiles (experimental studies, (HALL et al., 1975), SPIZZICHINO et VAN GRUNDERBEECK (1977)), at the same height ; but in theoretical studies, TELFORD (1970) finds 0.6 Z_I . This greater height of maximum may be caused by the hypothesis of a zero heat flux at Z_I , whereas experimentally negative heat flux below the inversion (to heights of the order of 0.7 Z_I , even 0.5 Z_I) is quite apparent (KAIMAL et al. 1976, ANDRE et al. 1978, WEILL et al. 1980) ; so, the zero heat flux height is less than Z_I .

1° Proposal for a new normalization of plume velocity

The vertical profile of plume velocity is quasi-similar to the velocity variance profile $\overline{W'^2}$ (Z/Z_T), with a maximum near $Z_T/3$. It has previously been shown (PANOFSKY (1978), McBEAN and McPHERSON (1976)) that, using similarity theory, the velocity variance is connected to the local mechanical and buoyancy production. By applying similarity principles to an individual plume, the mechanics of the plume would be directly determined by an elementary sensible heat transferred in it.

A new normalization of plume velocity is proposed :

$$\overline{W'^3}/Z = A \frac{g}{T_0} \overline{\theta'W'_p} \quad \text{in the Well Mixed Layer (W.M.L.)}$$

where, A universal constant (A = 1.86 as in velocity variance normalization suggested by WEILL et al. (1980). We give later a justification of this choice).

$\overline{W'\theta'_p}$ elementary sensible heat flux of the plume.

In dry W.M.L., the heat flux of the plume is supposed to decrease linearly with height, like the heat flux in the whole convective cell.

$$\text{Hence, } \overline{W'_p^3}/Z = 1.86 \frac{g}{T_0} \overline{\theta'W'_p} (1 - Z/h) \text{ in W.M.L.}$$

where $\overline{\theta'W'_p}$ is the surface temperature flux and h the height at which the heat flux vanishes by linear extrapolation.

This assumption is justified from observation since convective updrafts seem to play an active and important role in transporting heat and momentum from the surface layer. From HALL et al (1975), plume bases are localised region of great structure functions of temperature fluctuations (C_T^2). Plumes are bulk motions of warm air, of significant heat flux and turbulent momentum transfer (KAIMAL, 1976 - PALMER and CAUGHEY, 1978). From our study of TELFORD's model, 70 % of the surface heat flux is carried by plumes only.

2° Experimental verification of plume velocity normalization

To validate it, we must confirm the parabolic profile of $\overline{W'_p^3}$ with height in the W.M.L. and compare magnitudes of plume elementary heat flux obtained and mean heat flux computed by other probes. The following method is presented :

a) Linear decrease of $\overline{W_p^3}/Z$ in the W.M.L.

From experimental vertical profiles of $\overline{W_p^3}/Z$ in the convective layer, we test in the W.M.L. on at least 6 altitudes (depth of W.M.L. ≈ 100 m), quadratic deviations from a linear variation. We estimate, when the correlation is good, the surface plume heat flux Q_p , the reference height h , interesting to compare with the inversion height, (cf. fig. 18 and table 6 for the 32 successive plumes of the observed field).

On the 32 observed plumes, the correlation coefficient is larger than .9 for 12 plumes (corresponding to a relative statistical uncertainty $\frac{\Delta Q_p}{Q_p} < 20\%$) and the correlation coefficient for 18 plumes is larger than .8 ($\frac{\Delta Q_p}{Q_p} < 30\%$ and h/Z_I close to .7).

The normalized expression of $\overline{W_p}$ agrees well with experimental results, but the equation, derived for the well mixed adiabatic layer, does not take into account entrainment effects nor divergence of radiative flux, so h is different from the height where the plume heat flux really vanishes, but of a near magnitude.

Notice that 50 % of the 32 plumes were sharp edged. Their computed Q_p represent 70 % of the total added Q_p . Hence plumes with sharp edges are associated with the more energetic and active ones.

b) Comparison between elementary heat flux in plumes and mean heat flux

The surface heat flux Q_o was computed for a time period of 20 or 30 mn by sodar velocity variance profiles and for 1 hr using the BEARN system (INRA). INRA measurements are always a little lower than sodar, but within the discrepancy between the Q_o computations of all the various probes measuring it. Fig. 19 reveals the temporal variation of Q_o associated with individual contributions of surface heat flux Q_p in plumes.

A quasi constant ratio is found between surface heat flux contributions of plumes only, averaged on the same period, and Q_o measurements.

$\frac{Q_o \text{ by plumes}}{Q_o \text{ INRA}} = 60 \% \quad \text{within } \pm 10 \% \text{ scattering}$	}	Table 7
$\frac{Q_o \text{ by plumes}}{Q_o \text{ SODAR}} = 50 \% \quad \text{within } \pm 10 \%$		

50 % of the 32 plumes are determined with great accuracy (sharp edge). They represent 70 % of the total Q_p transfer, thus, only 30 % surface plume heat flux is uncertain. Hence, an imprecision of $\pm 15 \%$ is caused by the sodar determination of plume boundaries.

Hence, plumes seem to carry a little more than half of the surface heat flux. It will be interesting to study downdraft by direct measurements of W' and θ' . Manton (1977) have found experimental contributions of downdraft to heat flux of around 50 %, near the surface layer top.

4.4 Turbulence plume intensity and plume size

1° Turbulence plume intensity

Turbulence intensity (or r.m.s. velocity turbulence) is the second order turbulent moment of each entity. For plume, $i_p^2 = \overline{(w_p - \bar{w}_p)^2}$

$$\text{for downdraft, } i_e^2 = \overline{(w_e - \bar{w}_e)^2}.$$

For WARNER and TELFORD (1963), turbulence intensities are not markedly different for each entity. PALMER (1978) gives values of a turbulence level indicator, greater in ascending than in descending air, except from engulfing motion at Z_I . According to TELFORD (70), $i_p - i_e$ and turbulent intensity is constant with height.

Experimental results

a) Plume turbulence intensity

As in TELFORD, a study of the most sharp edged plumes reveals a vertical profile of i_p quasi constant with height (order of magnitude, 0.4 to 0.8 m/s, for maximum plume velocity < 1 m/s) (fig. 20). With a parabolic variation of $w_p^3(z)$ and

TABLE 6

Q_p SENSIBLE HEAT FLUX CARRIED BY PLUMES

Date	Plume number	Hour	Duration mn s	Q _p w/m ²	co	$\frac{\Delta Q_p}{\Delta Q_p}$	ΔQ_{p2} w/m ²	h	h/Z ₁
July 6 7.15—8.19	1	7.28.36 7.38.12	10.34	18	0.99	7 %	1	107	0.7
	2	7.44.36 7.46.36	2.04	48	0.73	30 %	14	104	0.5
	3	7.48.36 7.54.16	5.20	47	0.95	15 %	7	134	0.7
	4	7.56.00 7.58.52	2.50	74	0.93	18 %	13	160	0.9
	5	7.59.36 8.02.20	3.24	83	0.52	40 %	33	183	0.9
	6	8.04.32 8.06.44	2.12	23	0.97	12 %	3	120	0.7
	7	8.09.16 8.12.44	3.28	27	0.82	29 %	8	100	0.6
July 6 8.24—9.29	1	8.34.20 8.38.32	2.12	12	0.93	18 %	2	141	0.9
	2	8.43.30 8.46.30	3.00	167	0.80	30 %	50	141	0.8
	3	8.48.30 8.52.30	4.00	19	0.80	30 %	6	177	0.9
	4	8.54.32 8.56.48	2.16	8	0.64	38 %	3	170	0.8
	5	8.59.20 9.01.12	1.52	Q _p no estimable					
	6	9.03.30 9.04.40	1.10	92	0.91	20 %	18	215	0.7
	7	9.07.20 9.09.20	2.00	29	0.76	33 %	9	237	0.8
	8	9.12.16 9.14.48	2.32	59	0.81	30 %	18	216	0.6
	9	9.15.16 9.17.00	1.44	74	0.73	34 %	25	224	0.6
	10	9.17.48 9.19.08	1.40	33	0.64	38 %	12	175	0.5
	11	9.21.12 9.22.52	1.40	52	0.74	34 %	18	236	0.6

Date	Plume number	Hour	Duration mn. s	Q_{p2} W/m ²	co	$\frac{\Delta Q_p}{\Delta Q_p}$	ΔQ_{p2} W/m ²	h	h/Z ₁
July 6 9.33→10.29	1	9.38.16 9.40.16	2.00	8	0.64	38 %	3	240	0.6
	2	9.40.18 9.42.40	2.22	57	0.77	33 %	19	309	0.8
	3	9.53.00 9.57.32	4.32	134	0.94	15 %	20	242	0.6
	4	10.03.12 10.04.32	1.20	140	0.66	38 %	50	267	0.5
	5	10.05.06 10.06.24	1.18	58	0.82	30 %	18	339	0.6
July 11 8.08→8.42	1	8.11.38 8.13.26	2.44	293	0.93	18 %	53	171	0.7
	2	8.15.30 8.17.54	2.24	54	0.90	20 %	11	196	0.8
	3	8.22.50 8.24.02	1.12	8	0.72	34 %	3	96	0.4
	4	8.25.10 8.26.06	0.54	17	0.66	38 %	6	141	0.5
	5	8.28.14 8.31.46	3.32	94	0.90	20 %	19	207	0.7
	6	8.32.34 8.33.06	1.28	60	0.81	30 %	18	142	0.5
	7	8.33.50 8.35.02	1.12	271	0.90	20 %	54	195	0.7
	8	8.36.02 8.38.08	2.04	452	0.94	15 %	68	259	0.9
	9	8.38.42 8.39.58	1.16	16	0.40	45 %	7	240	0.8

TABLE 7

COMPARISON HEAT FLUX :SODAR ESTIMATE, I.N.R.A. ESTIMATE AND HEAT CARRIED BY PLUMES

Date	Hour	Duration	Q_o sodar W/m ²	Q_o INRA in terpolation W/m ²	Q_o plumes W/m ²	% Q_o sodar	% Q_o INRA
July 6	7.50	20 mn	57	57	29	50	50
	8.00	20 mn	69	58	37	53	64
	8.45	20 mn	75	60	32	43	53
	9.12	20 mn	62	56	29	47	52
	9.50	30 mn	55	44	30	54	70
	9.52	30 mn	55	43	33	60	77
July 11	8.20	20 mn	115	104	32	30	31
	8.30	20 mn	115	110	82	71	74

a constant value of $i_p(Z)$ in a well mixed layer, the turbulence rate in plume $\frac{i_p}{W_p}(Z)$ would exhibit a very flat minimum around 0.3, 0.4 Z_1 .

Experimental sodar results are in good agreement with this prediction (cf. fig. 21) :

from 0.2 up to 0.7 Z_1 , $\frac{i_p}{W_p}(Z) \approx 75 \% \pm 20 \%$

The turbulence level $\frac{i_p}{W_p}$ is half of the kinetic energy $(\overline{W_p^2})$ of the plume.

b) Downdraft turbulence intensity

Results are less conclusive. Downdraft areas are identified with less accuracy from our sodar record. Between two unambiguous sharp-boundaried plumes, successive ill defined plume may exist (cf. fig. 15), so in the intervening regions, downdraft with low vertical speeds are difficult to locate. Periods of intense downward motions are less frequent than upward (1 for 3). So they are not easy to detect by themselves.

The suggested findings are the following :

In early morning, with important height variation of Z_1 (7 h to 9 h 30), downdraft characteristics are very near those of updraft (similar vertical profile for $\overline{W_e}$, i_e , $\frac{i_e}{W_e}$). Periods of downdraft are often intense, perhaps connected to the quick rise of inversion layer. The rate of turbulence is constant in W.M.L., near 75 %, but i_e is slightly lower than the magnitude of i_p .

In later morning (with $Z_1 \approx 600$ m), the velocity pattern show longer periods of descending air of smaller variability. The magnitude of i_e is lower than i_p , but W_e is very weak, so the turbulence rate seems near 200 %. This study must be pursued for deeper convection.

2° Plume size and horizontal cross-section of up and downdrafts

From KAIMAL's et al. (1976) spectral study, length scale of plumes would be near 1.5 Z_1 : but sodar measurements of plume size (constant size with height) are strongly scattered with magnitude < 200 m. Nothing is concluded (fig. 22) : there is no contradiction with KAIMAL et al. for plumes diameter smaller this 500 m, but for larger plumes we need more results. The experimental computations of R, (the ratio between horizontal size of up and downdrafts (with TAYLOR hypothesis)) are of large variability (fig. 23) :

$$R = \frac{S_{\text{updraft}}}{S_{\text{downdraft}}} = \begin{cases} \left\{ \begin{array}{l} 0.2 < R < 0.8 \\ 0.2 < f < 0.4 \end{array} \right. & \text{for plume size} < 500 \text{ m} \\ \left\{ \begin{array}{l} 0.8 < R < 2.0 \\ 0.4 < f < 0.7 \end{array} \right. & \text{for plume size between} \\ & 500 \text{ and } 1500 \text{ m} \end{cases}$$

The simple and original assumption of a constant fraction f of the area occupied by convective elements, as modelled by MANTON (1975) does not seem to be supported by observations.

3° Phenomenological validation of the velocity normalization in plumes

The proposed normalization was asserted by restriction of similarity laws to an individual plume and experimental observation of turbulent patterns. Furthermore, a validation of the choice of the same universal constant as in normalized velocity variance W'^2 formulation, is proposed ($A = 1.86$).

The average distribution function inside and outside the plumes is fairly well approximated by a normal distribution, from VAN GRUNDERBEECK et al. (1979) and our entity averaged histograms (fig. 24): discrepancies are around 15 % for 30 %. We relate average turbulent moments (\bar{W} , W'^2 , W'^3) to individual mean values of both entities. Thus, W'^2 on a convective cell is :

$$\overline{W'^2} = \frac{[\overline{W_e^2} + i_e^2] + R[\overline{W_p^2} + i_p^2]}{1 + R}$$

with $\bar{W} = 0 \implies \overline{W_e} = -R \overline{W_p}$.

From experimental data, in the well mixed layer, in early morning,

$$\frac{i_p}{\overline{W_p}} \approx \frac{i_e}{\overline{W_e}}, \quad \text{so } W'^2 = \overline{W'^2} R \left[1 + \left(\frac{i_p}{\overline{W_p}} \right)^2 \right].$$

With, $\left\{ \begin{array}{l} R = 0.7 (f = 0.4) \\ \frac{i_p}{\overline{W_p}} \approx 75 \% \end{array} \right.$

$$\overline{W'^2} = \overline{W_p^2} \times C$$

$$C \approx 1.1$$

TABLE 8

C VARIABILITY AROUND UNITY

f	0.2	0.3	0.4	0.4
i_p/\bar{w}_p R	0.3	0.5	0.6	0.7
50 %	C VALUES 0.37	0.62	0.75	0.87
60 %	0.40	0.68	0.81	0.95
70 %	0.45	0.74 $\Delta = 26 \%$	0.89	1.04
75 %	0.47	0.78	0.94 $\Delta = 6 \%$	1.09
80 %	0.49	0.82	0.98	1.15 $\Delta = 15 \%$
90 %	0.54	0.90	1.09	1.27 $\Delta = 27 \%$
100 %	0.60	1.00	1.12	1.40

Δ = imprecision

Hence, plume velocity will have the same normalized formulation as velocity variance, with the same universal constant.

Table 8 reveals little variability of C around unity (at most 25 %) when R fluctuate between 0.5 to 0.7 and the turbulence rate from 70 % to 90 %.

5. CONCLUSION

We have shown that convective activity is responsible of a dissymmetry in the distribution function of vertical velocity : this skewness has been found to be well normalized using the convective velocity W_* .

It has been found that updraft and downdraft correspond to two families of vertical velocity distribution function.

With cautions and drastic tests we have presented an acoustic sounder method for plume determination in the well mixed layer, from the top of the surface layer, and a comparison between MANTON's (1975) and TELFORD's (1979) modelling has allow us to validate some characteristics of plumes variables using acoustic Doppler sounder.

- the mean velocity is found to be parabolic.
- the heat flux carried by elementary thermal plume is suggested to be near 60 % of the whole surface heat flux.
- the plume size seems to be different from $1.5 Z_1$, at least in the case of shallow convection in the morning.
- the turbulent intensity associated with updrafts and downdrafts appears to be constant in the well mixed layer.

A phenomenologic validation of our results has been added.

Specific measurements of descending air (plumes and downdraft) are required to elaborate transfer mechanics between the two entities. Systematic observations of more fully developed convection (for $- Z_1/L \geq 10$) would be advisable.

This study will be the object of our future work : observation of convective structure using acoustic Doppler sodar (eulerian investigation) and spatial investigation. One of the fundamental study is indeed the transfer from the surface up to the free atmosphere and the physical significance and connection between surface layer flux and mixed layer flux : problem of spatial extension of flux measurement.

APPENDIX

Potential heat flux contribution of updraft and downdraft

TELFORD and MANTON consider the average potential heat flux transferred by the convective cells as a whole (updraft and surrounding downdraft). But it seems interesting to separate individual contribution of each motion. We use equation and variables of TELFORD model (1970) for this computation.

The average potential heat flux is :

$$Q_t = \overline{\theta'W'} = b^2(\theta_p - \bar{\theta})(W_p - \bar{W}) + (c^2 - b^2)(\theta_e - \bar{\theta})(W_e - \bar{W})$$

plume contribution Q_p downward contribution Q_e

b is the plume circular radius

c the total circular radius of the cell

θ' is the fluctuating part of the potential temperature, averaged here on a whole cell.

Thus, in the plume : $\theta'_p = \theta_p - \bar{\theta}$
 plume temperature averaged on the cell

This decomposition results of the statistically uniform interior of each entity. From TELFORD's equation (9), $\bar{W} = 0$ (no average volume flow).

From TELFORD we get

$$\frac{Q_p}{Q_t} = \frac{c^2 - b^2}{c^2} = \frac{\text{Surface of downward air}}{\text{Total surface}} = 1 - f \text{ plume}$$

with theoretical predictions of TELFORD's model :

$$\begin{array}{l} Z_o = 400 \text{ m} \\ \rho_o \rightarrow 1,5^\circ\text{K/hr} \implies f = 0.3 \implies \frac{Q_{\text{plume}}}{Q_t} = 0.7 = 70 \% \\ i_o = 1 \text{ m/s} \end{array}$$

Plumes would carry only 70 % of the surface heat flux. Downward surrounding air may have a positive contribution to the surface heat flux (30 %), perhaps by mechanics of lateral turbulent entrainment of air.

FIGURE CAPTIONS

Fig. 1 : Voves July 6, 1977. Schematic decomposition of facsimile record (Reflectivity and Doppler) connected with the mean micrometeorological characteristics of the convective boundary layer.

Fig. 2 : Morning evolution of inversion height Z_I , surface heat flux Q_0 , friction velocity U_* and instability parameters $-Z_I/L$ during VOVES EXPERIMENT, July 1977.

Fig. 3 : Part 1 $\overline{W'^3}$ profiles collected every 3 mn
Part 2 the $\overline{W'^3}$ profiles during three different time periods. (Averaging time is chosen as function of each field of convective cells).

Fig. 4 : Convective velocity as a function of time during VOVES 77 EXPERIMENT. (using either sodar, either I.N.R.A. measurements).

Fig. 5 : Vertical velocity skewness $\frac{\overline{W'^3}}{W_*^3}$ as a function of normalized height Z/Z_I .

Fig. 6 : (1) vertical velocity histogram, early morning (the figure shows the sliced histogram and histogram with gaussian curve fitting)
(2) histogram in developed convection.

Fig. 7 : July 6 (VOVES 77). The inversion height following (maximum of reflectivity) and filtering (6 mn and 20 mn).

Fig. 8 : The vertical sodar velocity as a function of Z/Z_I , choice of different averages (20 mn, 10 mn).

Fig. 9 : Voves experiment (percent of aberrant data as a function of height).

Fig. 10 : The vertical velocity histograms

(1) superposition of three gates (39 m, 73 m, 107 m)

(2) superposition of seven gates in the mixed layer between 39 m and 175 m.

The average is indicated in full line

(3) superposition of four histograms in the mixed layer between 43 m and 243 m
(July 2, 1977) 10 h 45 → 11 h 15.

The average is indicated in full line.

Fig. 11 : Histograms and dissymetry evolution. The top of the figure corresponds to July 2 and the bottom of the figure corresponds to July 6.

Fig. 12 : Comparison aircraft and sodar histograms.

Fig. 13 : Negative vertical velocity mode W_1 and positive vertical velocity mode W_2 as a function of W_* .

Fig. 14 : July 6 (1977) VOVES. Vertical velocity histogram in the well mixed layer. The W threshold corresponding to the plumes is indicated and the two velocity modes (negative and positive) are indicated.

Fig. 15 : The vertical velocity observed with the Doppler Sodar, the inversion height and the plumes as determined by the sodar criterium (July 11 (1977)).

Fig. 16 : Limitation of the plume by determination test : the W threshold is chosen between $.3 \text{ ms}^{-1}$ and 0.6 ms^{-1} .

Fig. 17 : Plume vertical velocity as function of normalized height Z/Z_I .

Fig. 18 : July 11 (1977). The sensible heat flux carried by plumes (Q_p the sensible heat flux, h the zero heat flux height, C_o the correlation of the mean square line estimate).

Fig. 19 : The sensible heat flux contribution of the plumes in the top of the surface layer, the Sodar sensible heat flux (average along 20 mn) and the INRA sensible heat flux (average along one hour).

Incertitude is indicated.

Fig. 20 : The turbulence intensity of plumes during July 6 and July 11, 1977 (VOVES) as function of the normalized height Z/Z_I .

Fig. 21 : July 6. Examples of velocity turbulence intensities in plumes, and normalized turbulent intensity.

Fig. 22 : Plumes dimension D as function of inversion height Z_I .

$D = 1.5 Z_I$ is indicated.

Fig. 23 : Ratio of updraft and downdraft surface as function of plumes dimensions.

Fig. 24 : Downdraft and updraft histograms, July 6 (VOVES).

Fig. 25 : The plumes characteristics (vertical velocity, sensible heat flux profiles, turbulence intensities) and the Voves July 6/1977 facsimile record.

REFERENCES

- André, J.C., G. De Moor, P. Lacarrère, and R. du Vachat, 1975 : Turbulence approximation for inhomogeneous flows : Part I. The clipping approximation, *J. Atmos. Sci.*, vol. 33, p. 476-481.
- André, J.C., G. De Moor, P. Lacarrère, G. Therry and R. du Vachat, 1978 : Modelling the 24-hour evolution of the mean and turbulent structures of the planetary boundary layer, *J. Atmos. Sci.*, 35, 1861-1883.
- Arnold, A., J.R. Rowland, T.G. Konrad, J.H. Richter, D.R. Jensen and V.R. Noonkester, 1975 : Simultaneous observations of clear air convection by a pulse radar, an acoustic sounder and an instrumented aircraft, Preprints 16th Radar Meteorology Conference, 22-23 April, Houston, Tex., *Amer. Meteor. Soci.*, 290-295.
- Chong, M., 1976 : "Mesure des profils de vent par sodar Doppler", Note Technique CRPE/22.
- Deardoff, J.W., 1974 : Three-dimensional numerical study of the height and mean structure of a heated planetary boundary layer, *Bound. Layer Meteor.*, 7, 81-106 and 199-226.
- Frangi, J.P., 1979 : Contribution à l'étude de la structure verticale des principales caractéristiques turbulentes de la couche limite planétaire, Thèse de 3ème cycle PARIS VII.
- Frisch, A.S., J.A. Businger, 1973 : A study of convective elements in the atmospheric surface layer, *Bound. Layer Meteor.*, 3, 301-328.
- Hall, F.F., J.G. Edinger and W.D. Neff, 1975 : Convective plumes in the planetary boundary layer, investigated with an acoustic echo sounder, *J. Appl. Meteor.*, 14, 513-523.
- Kaimal, J.C., J.C. Wyngaard, D.A. Haugen, O.R. Coté and Y. Izumi, S.J. Caughey and C.J. Readings, 1976 : Turbulence structure in the convective Boundary Layer, *J. Atmos. Sci.*, vol. 33, p. 2152-2169.

- Klapisz C. et A. Weill, 1978 : Modèle semi-empirique d'évolution matinale entre le sol et le sommet de l'inversion, *J.R.A.*, 12, 113-117.
- Konrad, T.G., 1970 : The dynamics of the convective process in clear air as seen by radar, *J. Atmos. Sci.*, 27, 1138-1147.
- McBean, G.A., and J.I. McPherson, 1976 : Turbulence above lake Ontario : Velocity and scalar statistics, *Bound. Layer Meteor.*, 10, 181-197.
- Manton, M.J., 1975 : Penetrative convection due to a field of thermals, *J. Atmos. Sci.*, 32, 2272-2277.
- Manton, M.J., 1977 : On the structure of convection, *Bound. Layer Meteor.*, vol. 12, n° 4.
- Palmer, S.G., and S.J. Caughey, 1979 : An observational study of entraining convection using balloon-borne turbulence probes and high-power doppler radar, *Bound. Layer Meteor.*, 16, 261-278.
- Panofsky, H.A., 1978 : Matching in the convective planetary boundary layer, *J. Atmos. Sci.*, 35, 272-276.
- Perrier, A., B. Itier, J.M. Bertolini and N.B. Katerji, 1976 : A new device for continuous recording of energy balance of natural surface, *Agric. Meteor.*, 16, 71-84.
- Spizzichino, A., 1974 : Discussion of the operating conditions of a doppler sodar, *J. Geophys. Research*, vol. 79, n° 36, p. 5585-5591.
- Spizzichino, A., P. Van Grunderbeeck, 1977 : Etude des plumes convectives de la basse atmosphère par sondage acoustic doppler, *Annales de Géophysique*, t. 33, n° 4, p. 399-407.
- Telford, J.W., 1970 : Convective plumes in a convective field, *J. Atmos. Sci.*, 27, 347-358.
- Van Grunderbeeck P., P. Leberre, A. Weill, G. Dubosclard, B. Itier, 1979 : Mouvements convectifs de la couche limite atmosphérique observés au moyen de sondeurs acoustiques Doppler et d'instruments portés par un ballon captif, *C.R. Acad. Sc. Paris*, t. 288, pp. 209-212.

Warner, J., and J.W. Telford, 1963 : Some patterns of convection in the lower atmosphere, *J. Atmos. Sci.*, 20, 313-318.

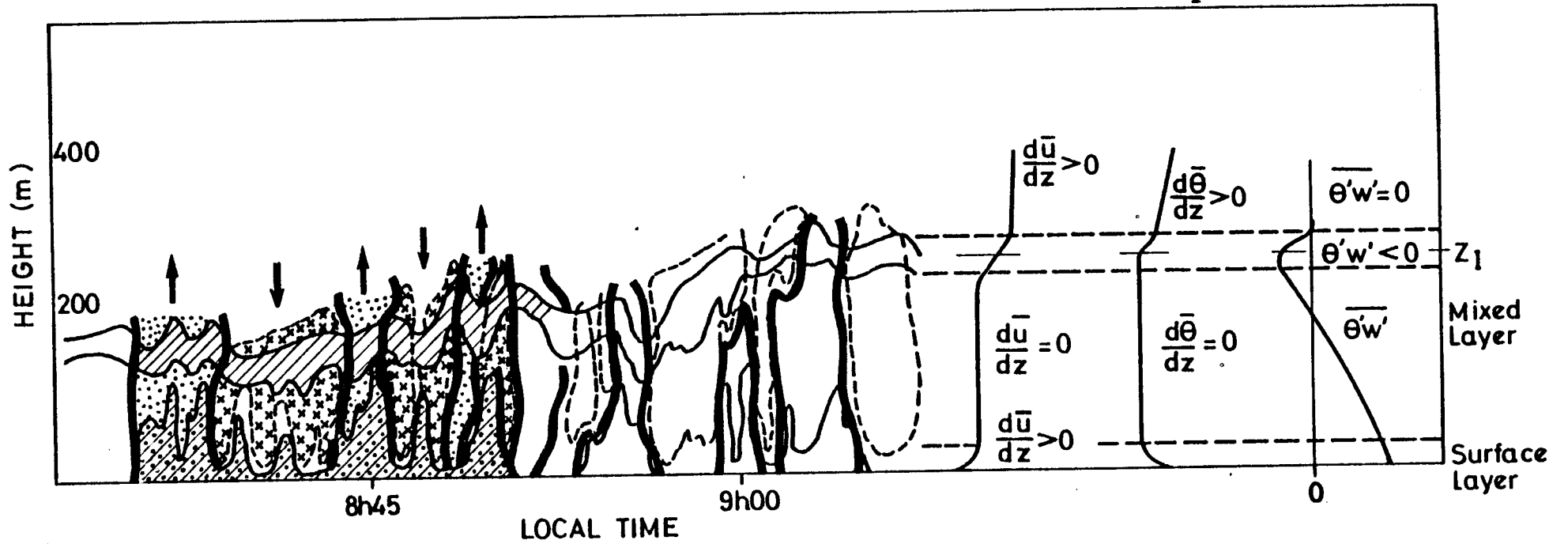
Warner, J., and J.W. Telford, 1967 : Convection below cloud base, *J. Atmos. Sci.*, 24, 374-382.

Weill, A., M.E. Le Quere, P. Van Grunderbeeck, J.P. Goutorbe, 1978 : Measurements of vertical velocity variance by means of an acoustic sounder, Fourth symposium on meteorological observations and instrumentations, Denver, Colorado, American Meteor. Soci., April 78, p. 459-460.

Weill, A., F. Baudin, J.P. Goutorbe, P. Van Grunderbeeck et P. Leberre, 1978 : Turbulence structure in temperature inversions and in convection fields as observed by Doppler Sodar, *Boundary Layer Meteorology*, 15, 375-390.

Weill, A., C. Klapisz, B. Strauss, F. Baudin, C. Jaupart, and P. Van Grunderbeeck and J.P. Goutorbe, 1980 : Measuring heat flux and structure functions of temperature fluctuations with an acoustic doppler sodar, *J. Applied Meteorol.*, vol. 19, n° 2, February, 199-205.

VOVES 06-07-77






-  REFLECTIVITY
-  UPWARD VELOCITY
-  DOWNWARD VELOCITY

FIG. 1

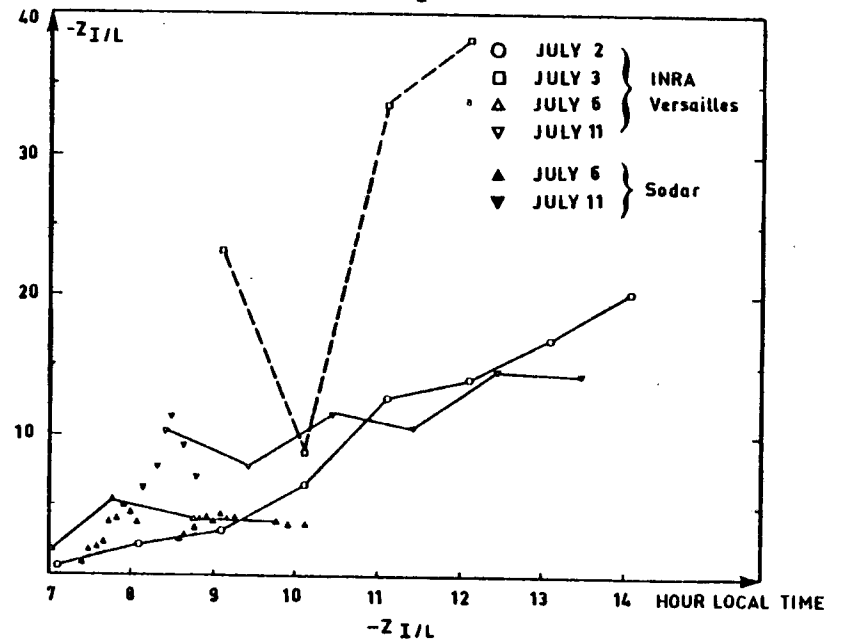
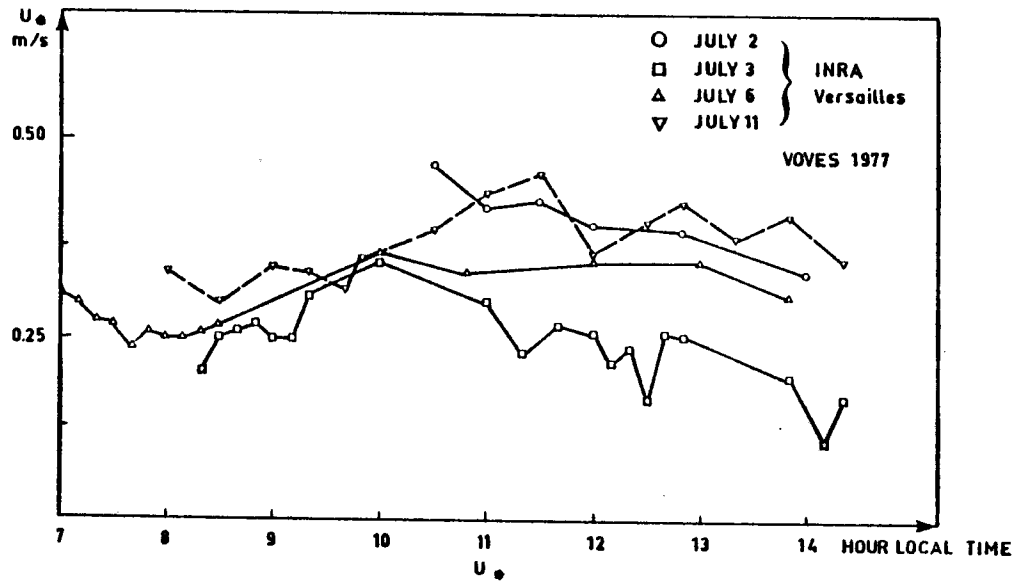
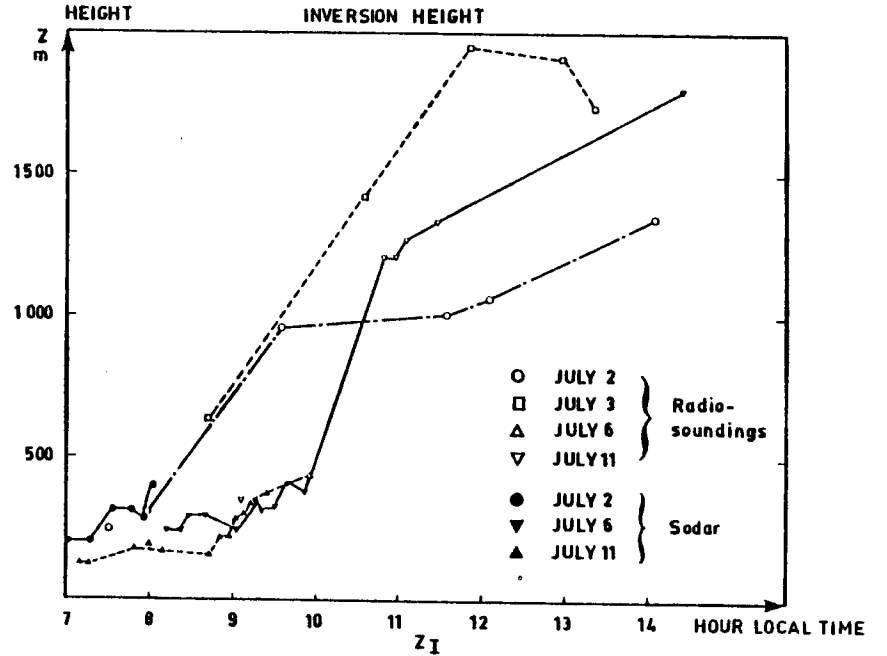
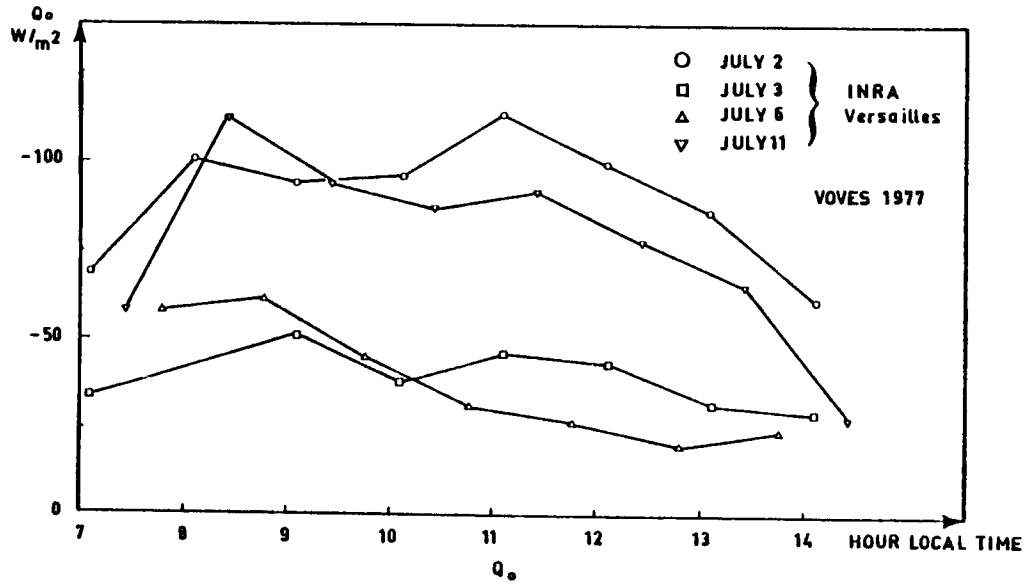


FIG.2

- 8.58
- 9.01
- + 9.04
- x 9.07
- 9.10
- 9.13
- △ 9.16

VERTICAL VELOCITY THIRD ORDER MOMENTUM

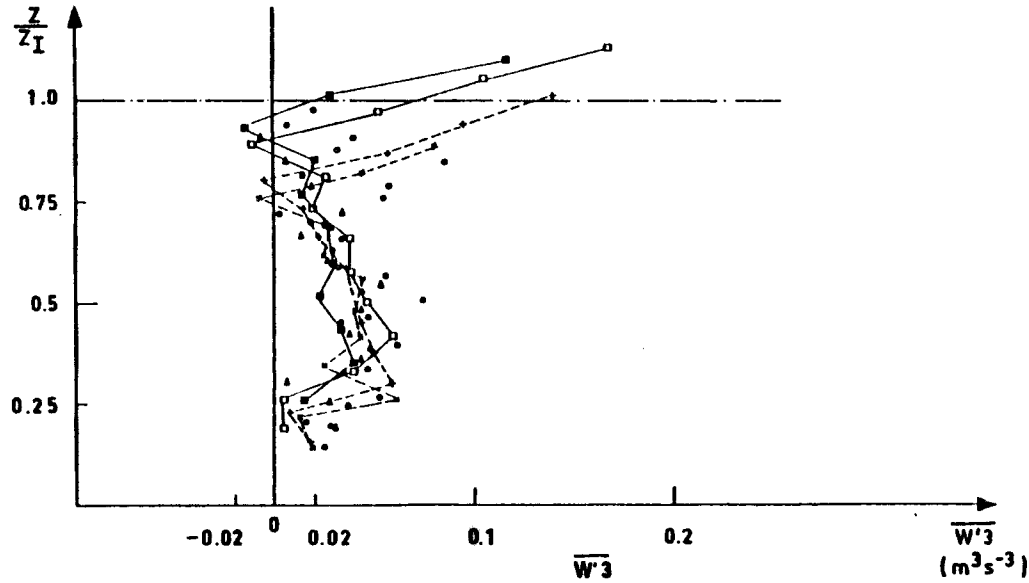
- 1: 7.15 ÷ 8.19
20mn.
▽□○△

2: 8.24 ÷ 9.29
20mn.
▼■●▲◆

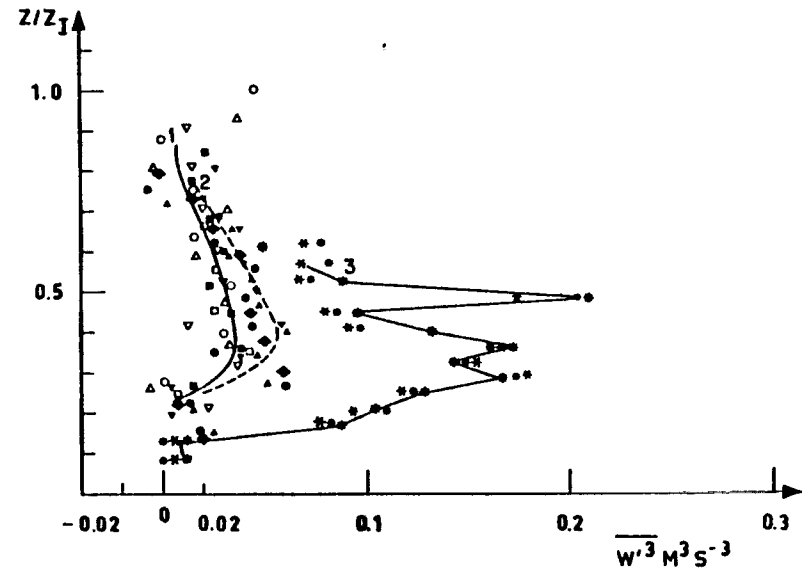
3: 9.33 ÷ 10.29
30mn.
* * *

Voves
JULY 6 (1977)

JULY 6 (1977) VOVES



(1)



(2)

FIG.3

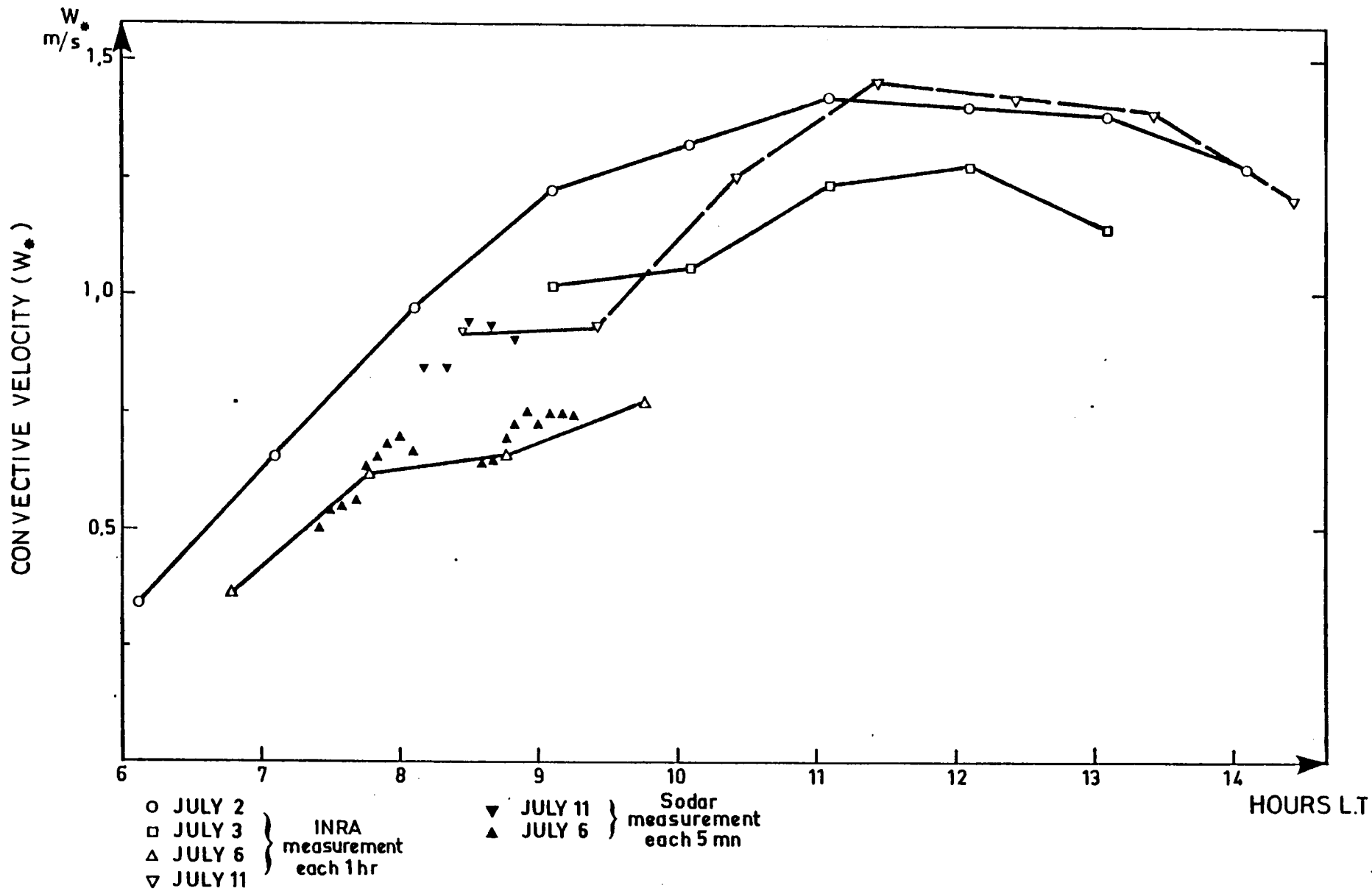


Fig. 4

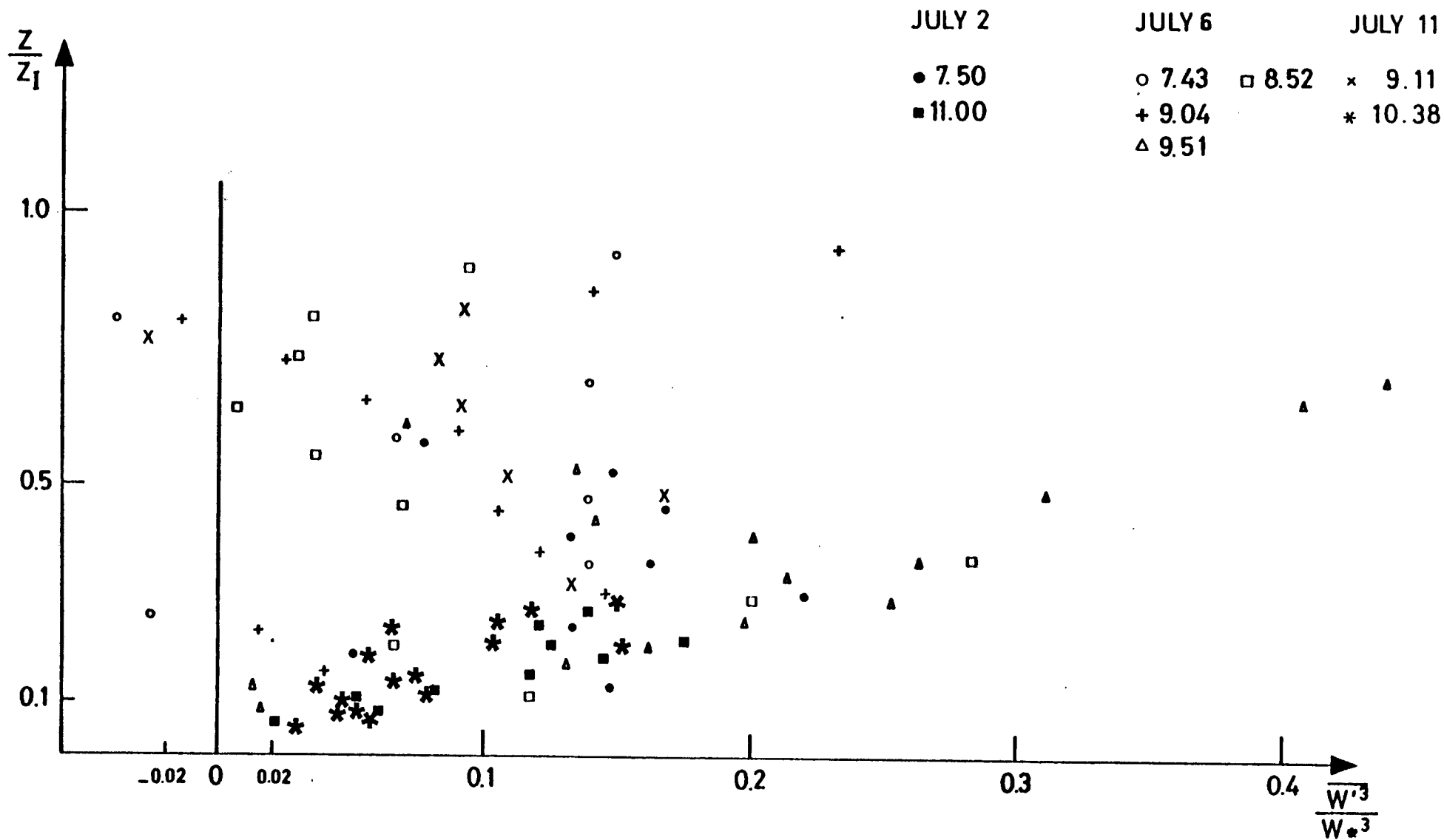
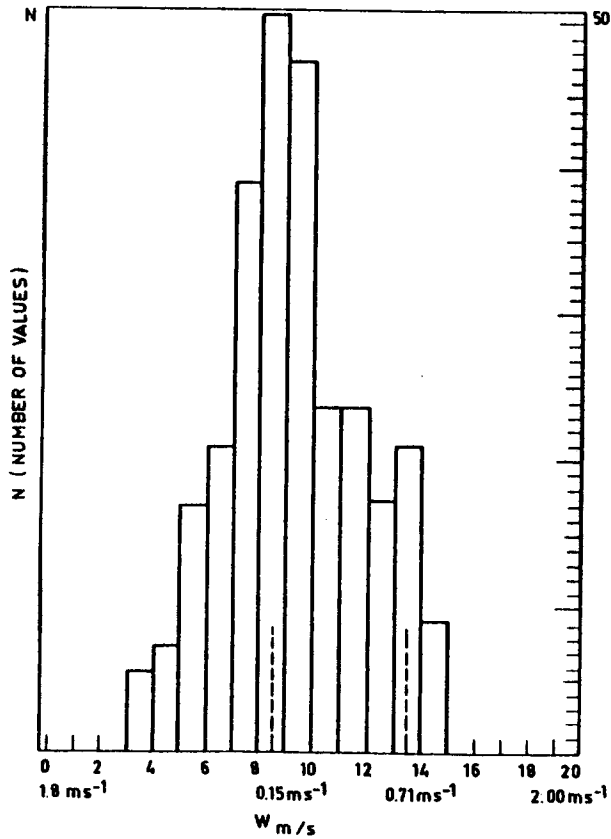


Fig. 5

JULY 6 (1977) VOVES

8.51 9.11

Z = 73m = 0.3 Z₁



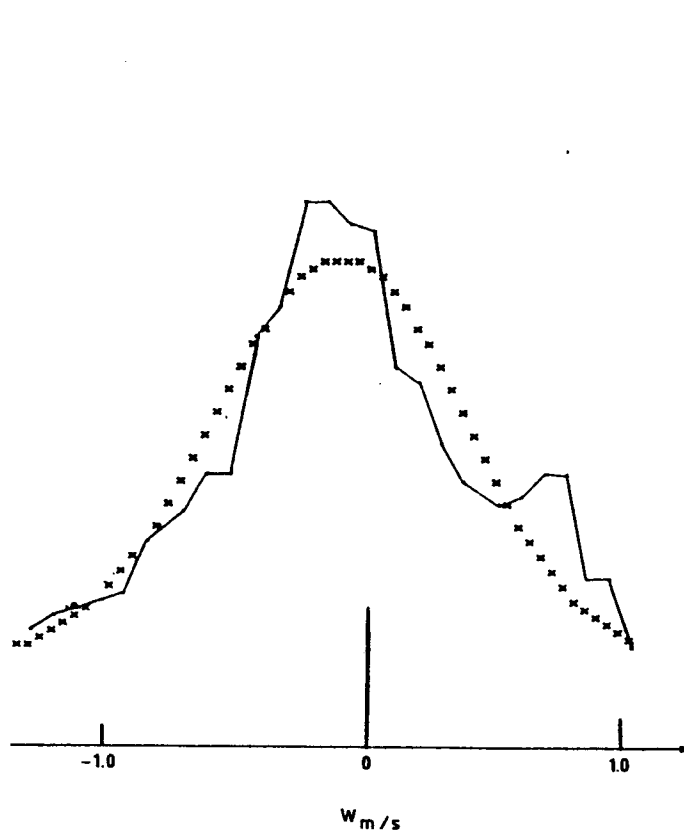
histogram

part 1

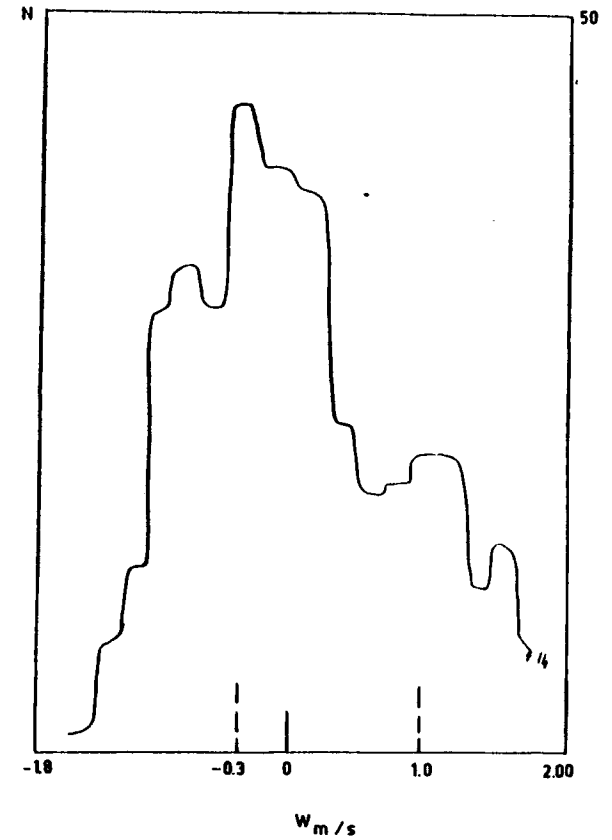
JULY 2 (1977) VOVES

10.45 11.15

Z = 243m = 0.2 Z₁



normal distribution
curve fitting



part 2

Fig. 6

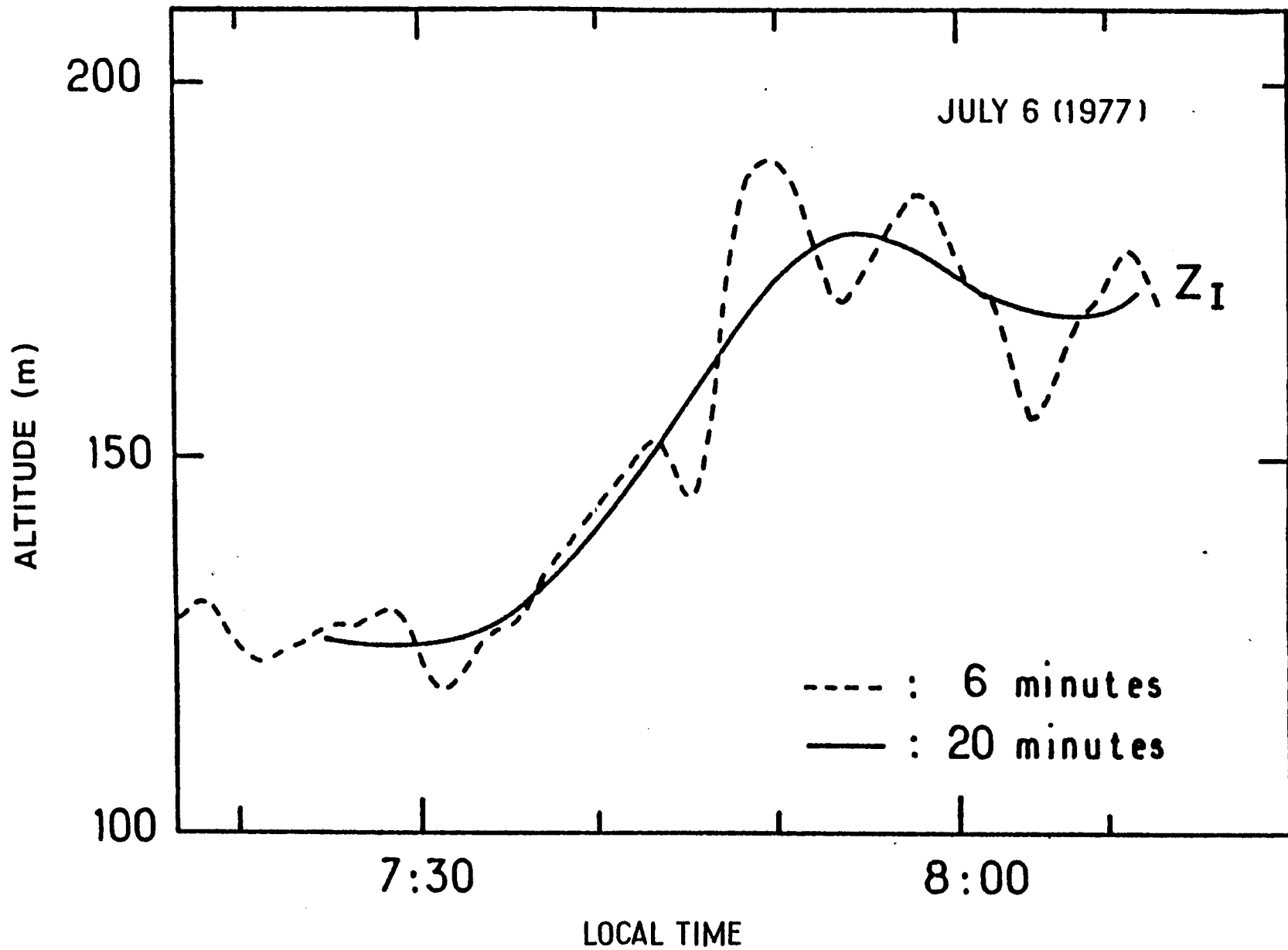


Fig. 7

JULY 6 (1977) VOVES

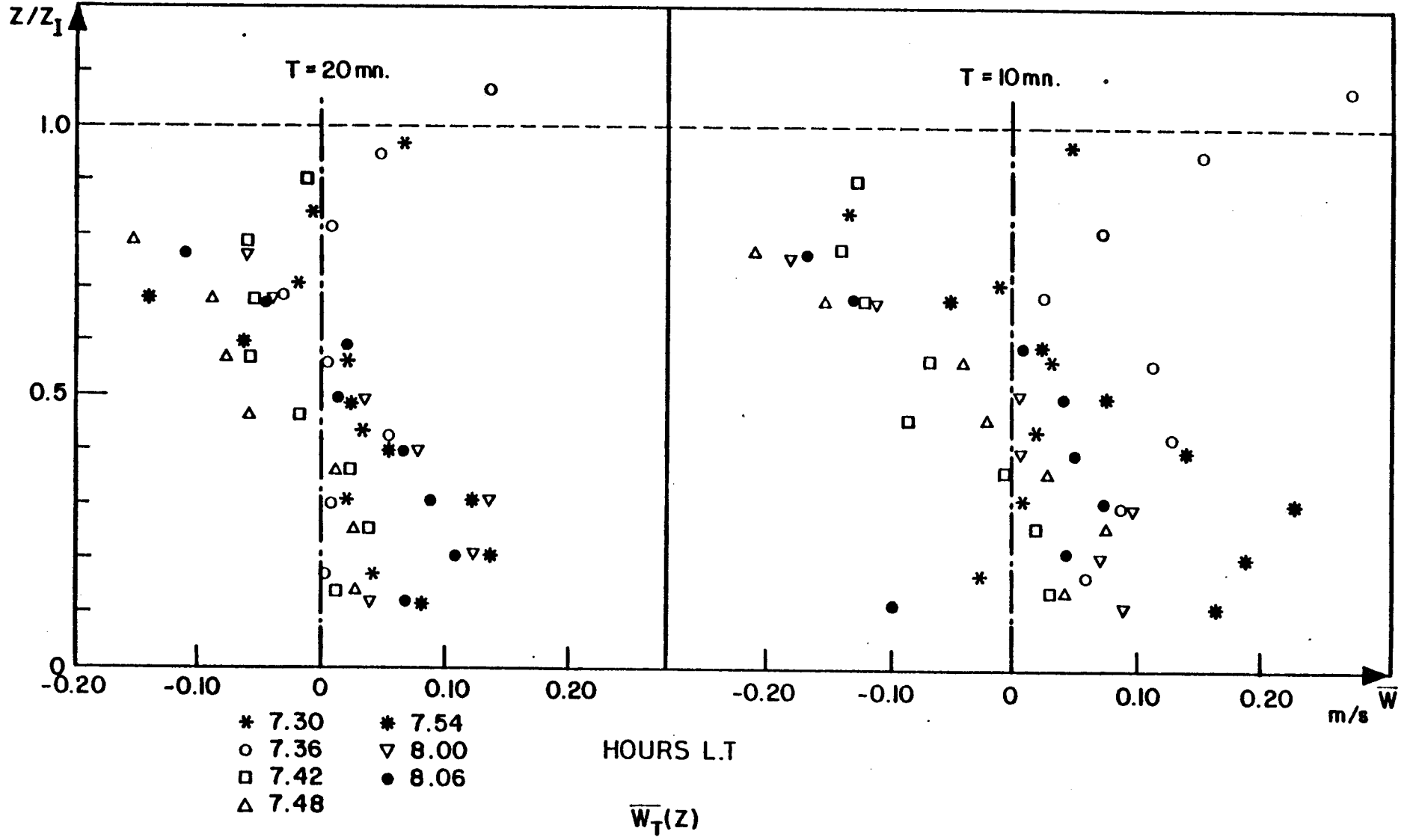


Fig.8

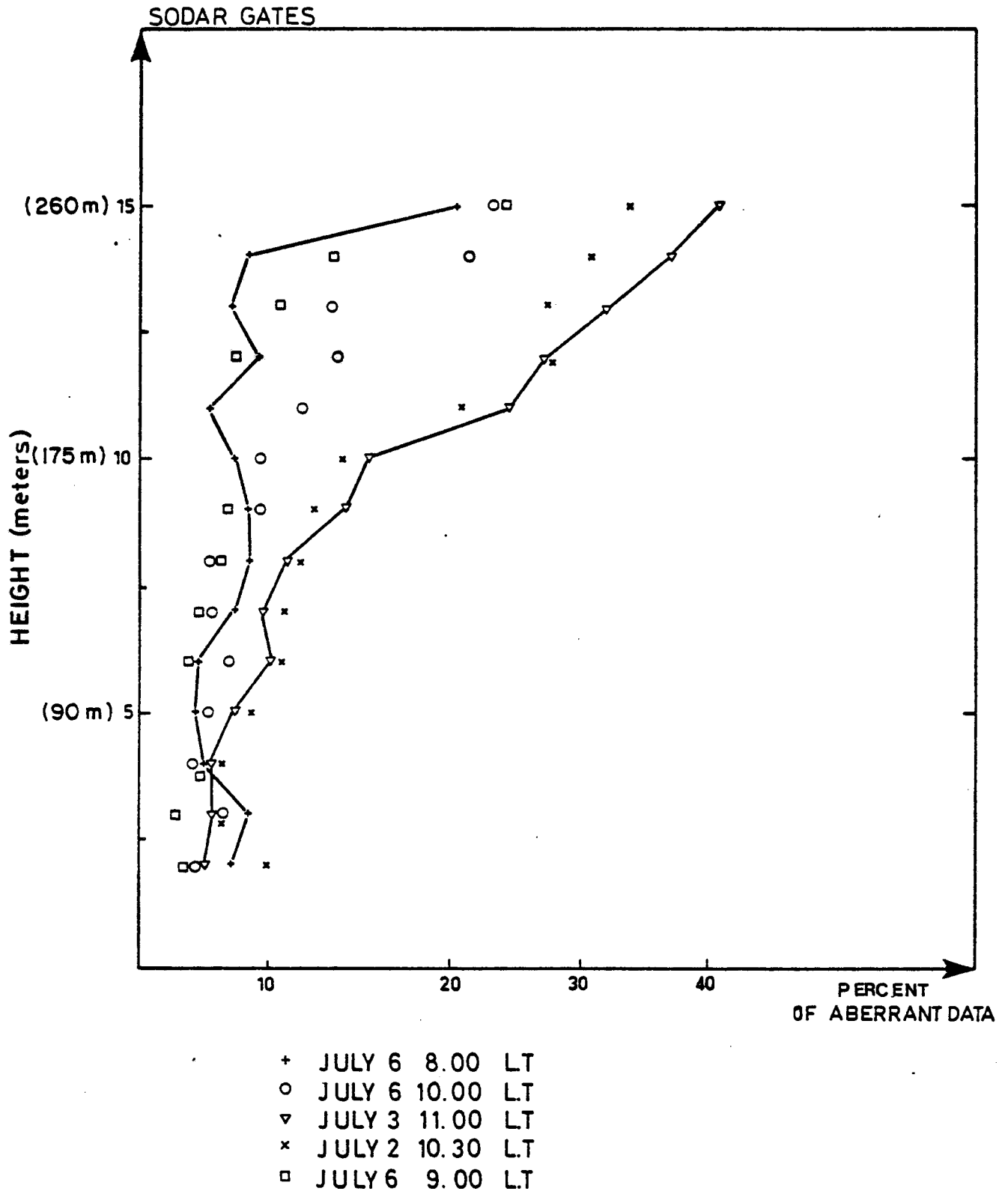
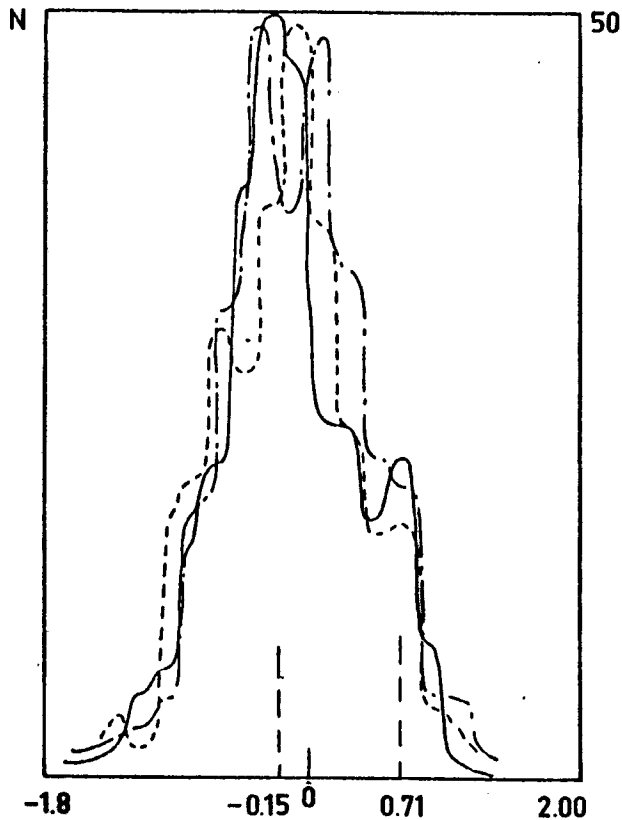


Fig.9

JULY 6 (1977) VOVES
8.51 → 9.11

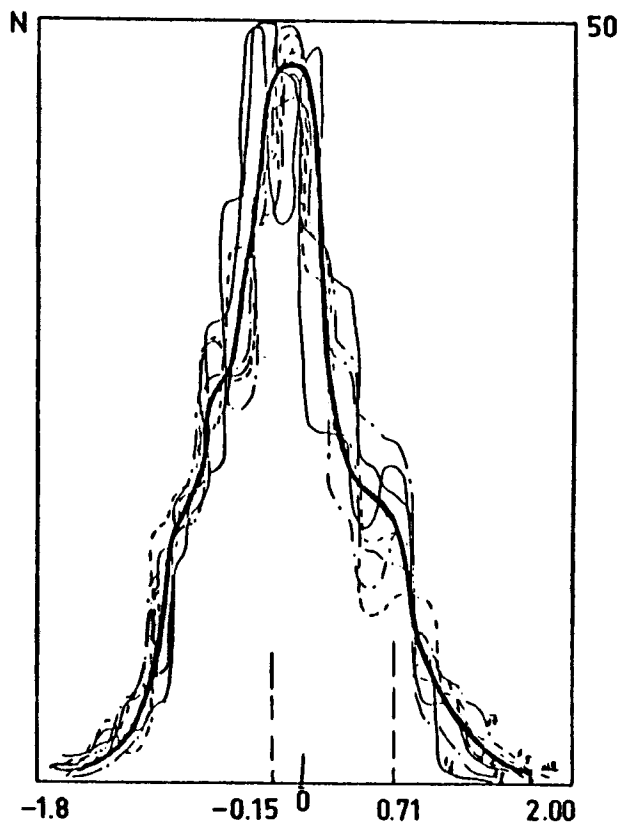


$Z = 39\text{m} (0.17 Z_I)$
 $Z = 73\text{m} (0.30 Z_I)$
 $Z = 107\text{m} (0.46 Z_I)$

$W_{\text{m/s}}$

(1)

JULY 6 (1977) VOVES

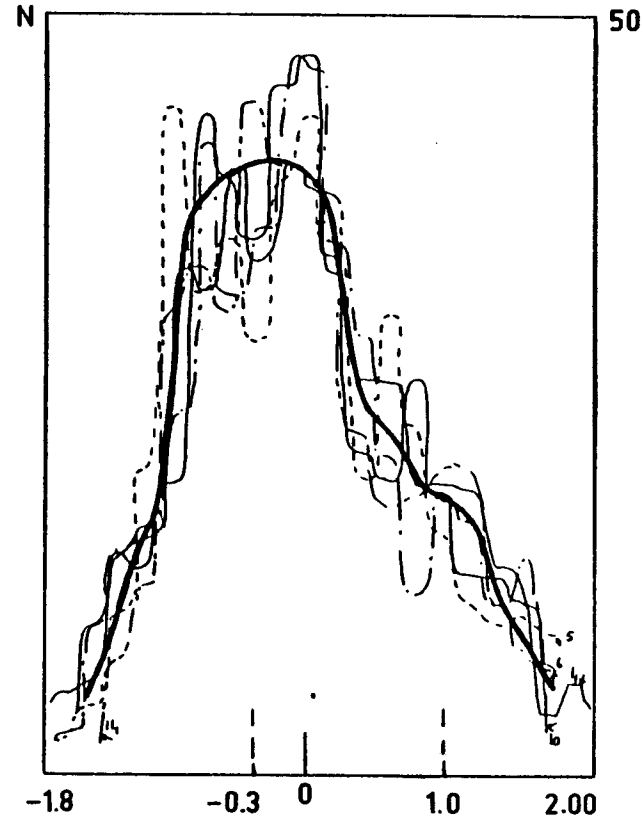


$Z = 39\text{m} \rightarrow Z_I = 175\text{m}$

$W_{\text{m/s}}$

(2)

JULY 2 (1977) VOVES
10.45 → 11.15



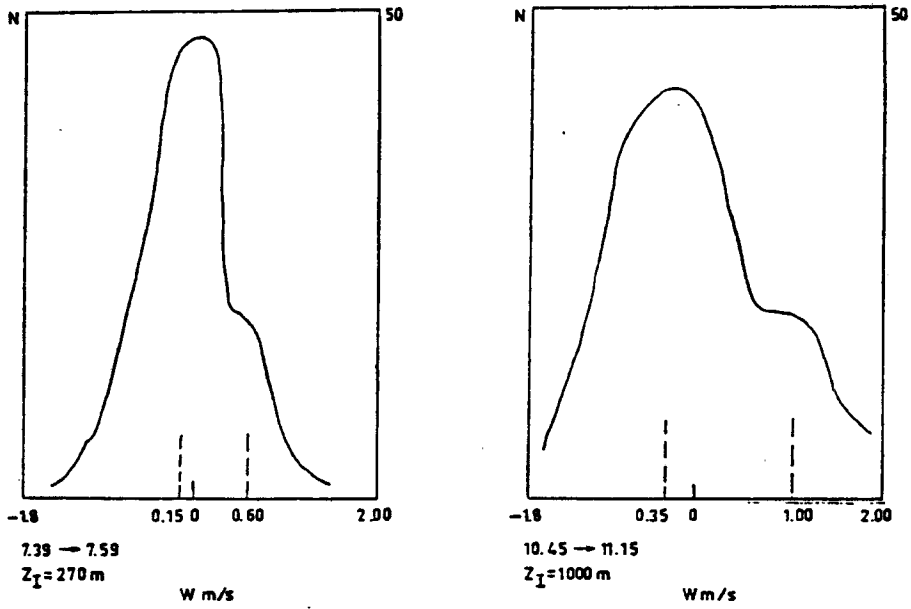
$Z = 43\text{m} \rightarrow Z_I = 243\text{m}$

$W_{\text{m/s}}$

(3)

Fig. 10

JULY 2 (1977) VOVES



JULY 6 (1977) VOVES

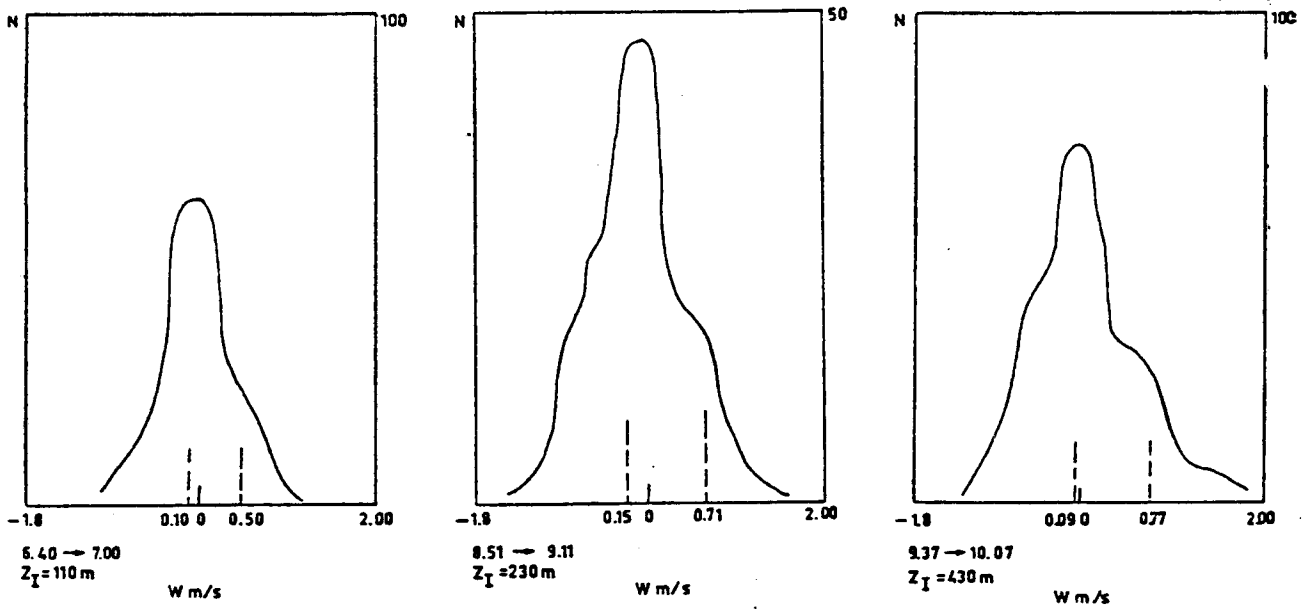


Fig.11

COMPARISON AIRCRAFT-SODAR HISTOGRAMS

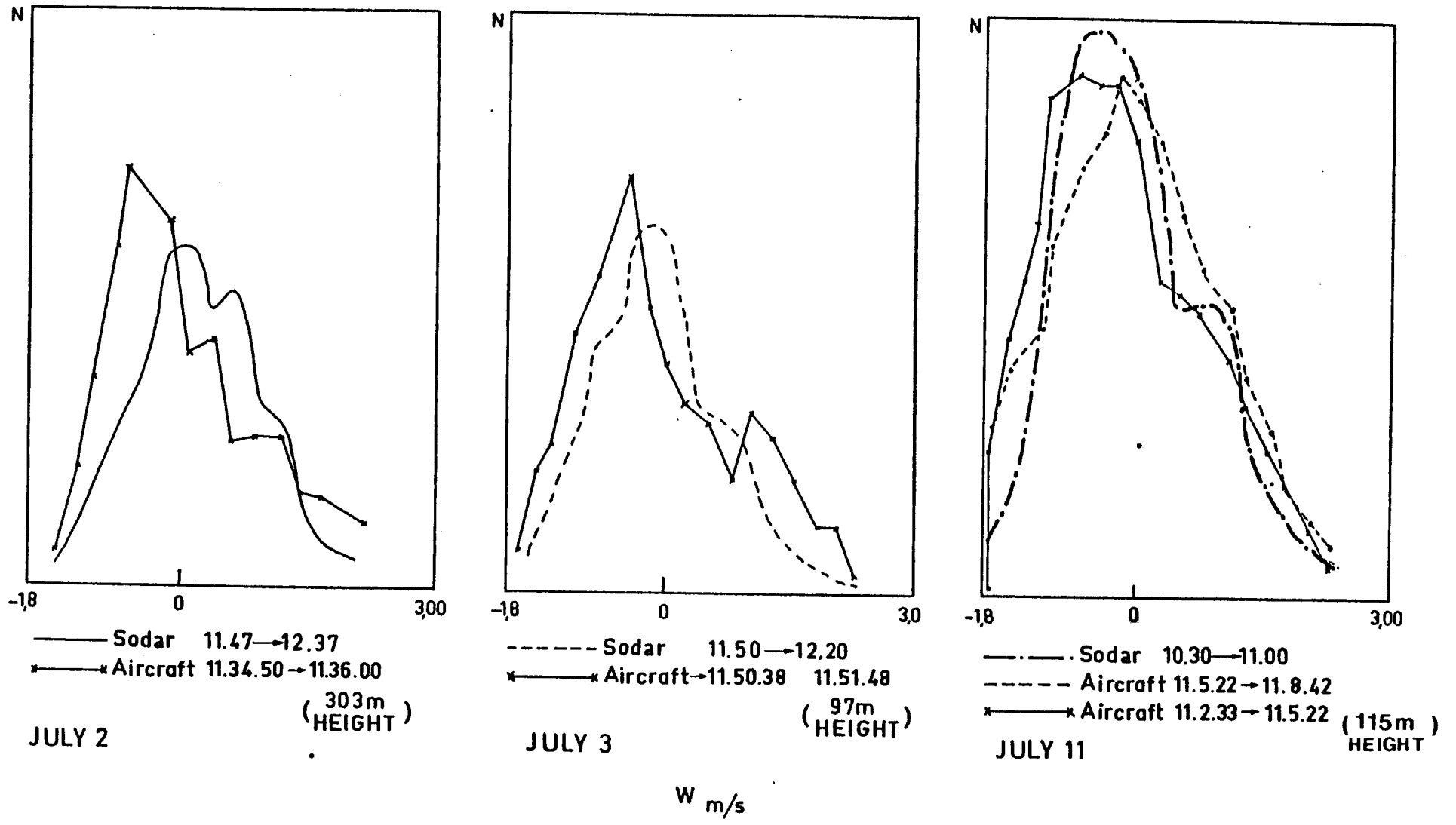


Fig. 12

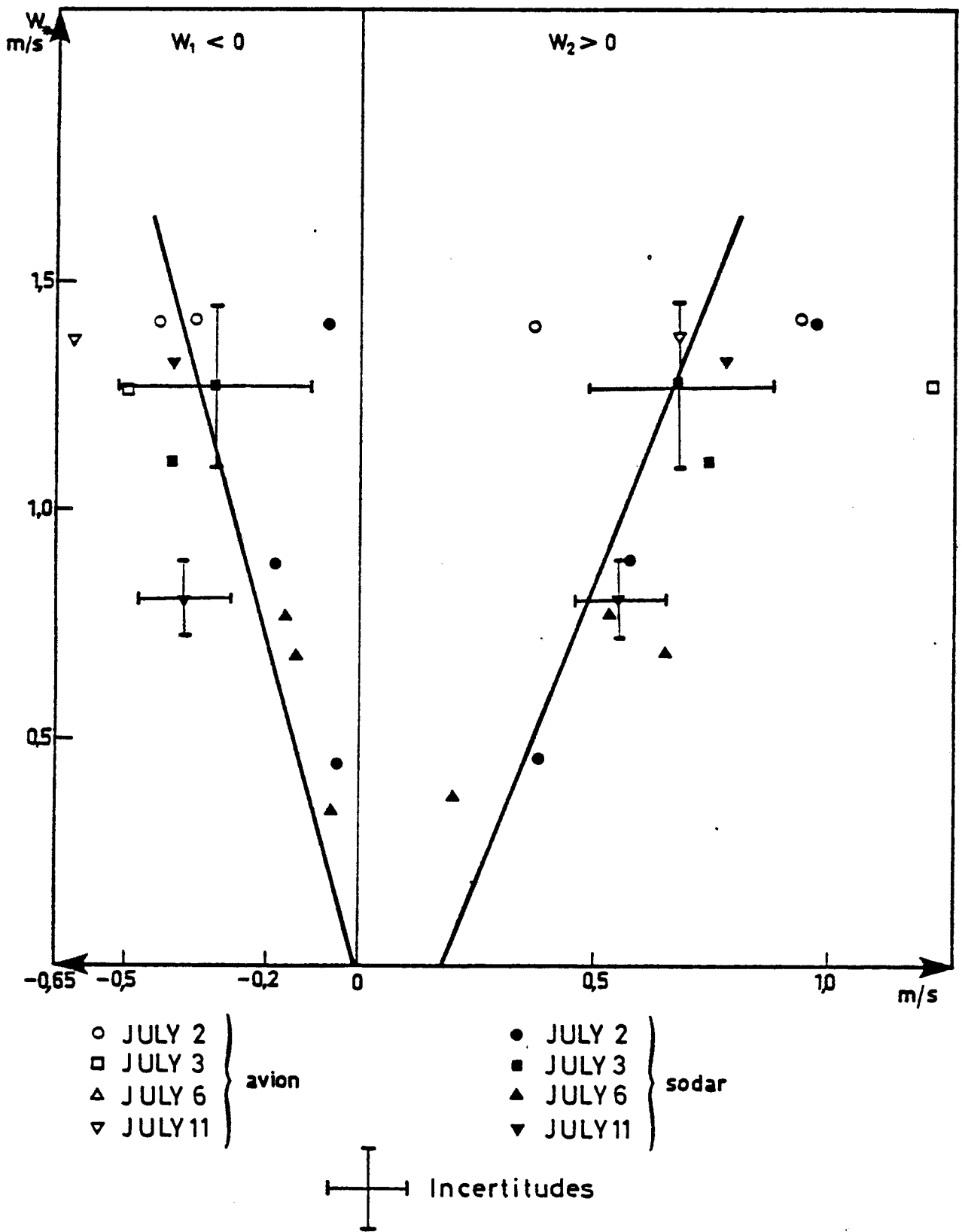


Fig. 13

8.51 → 9.11
 $Z_I = 230\text{ m}$

JULY 6 (1977) VOVES
HOURS LT

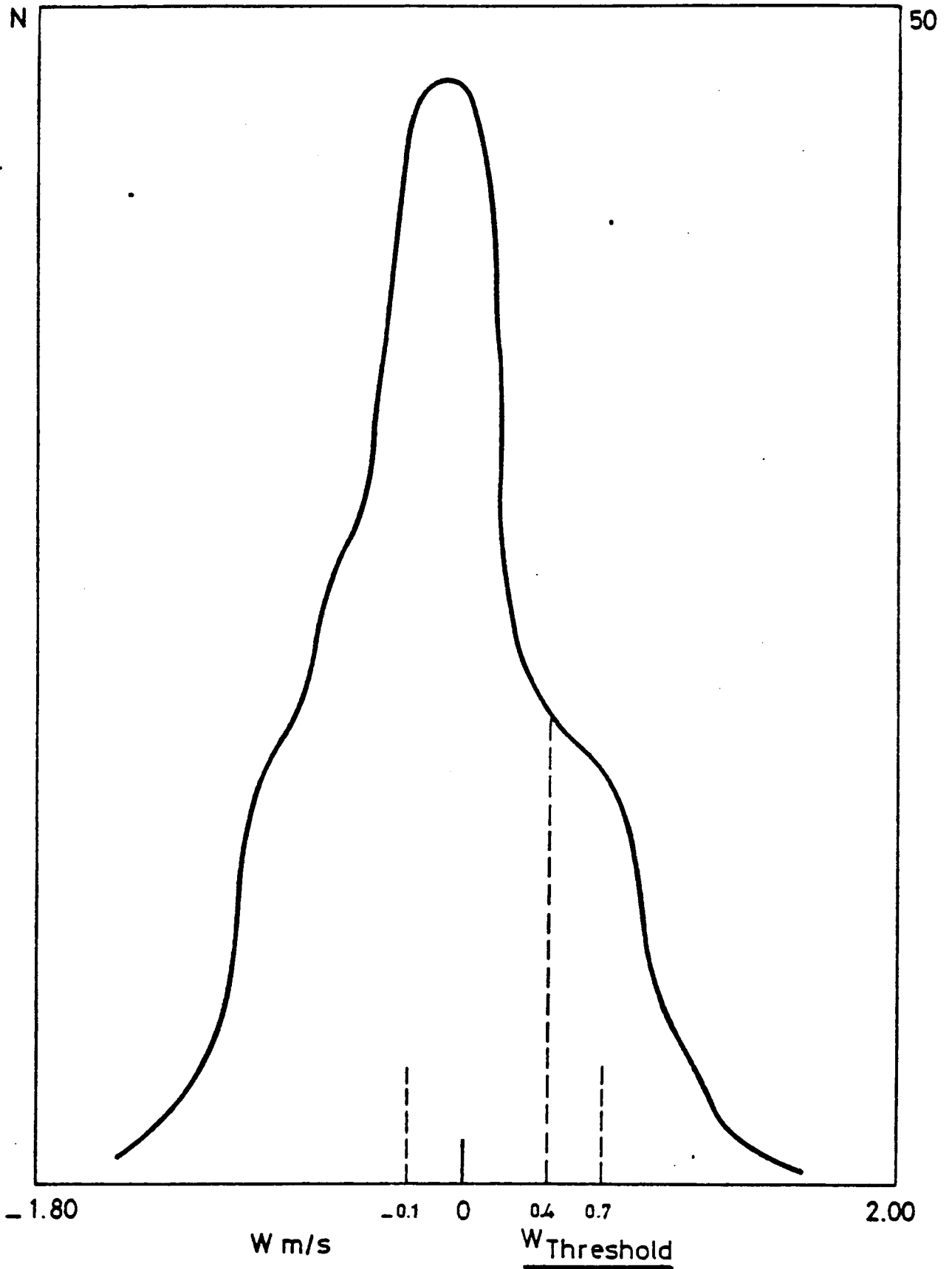


Fig.14

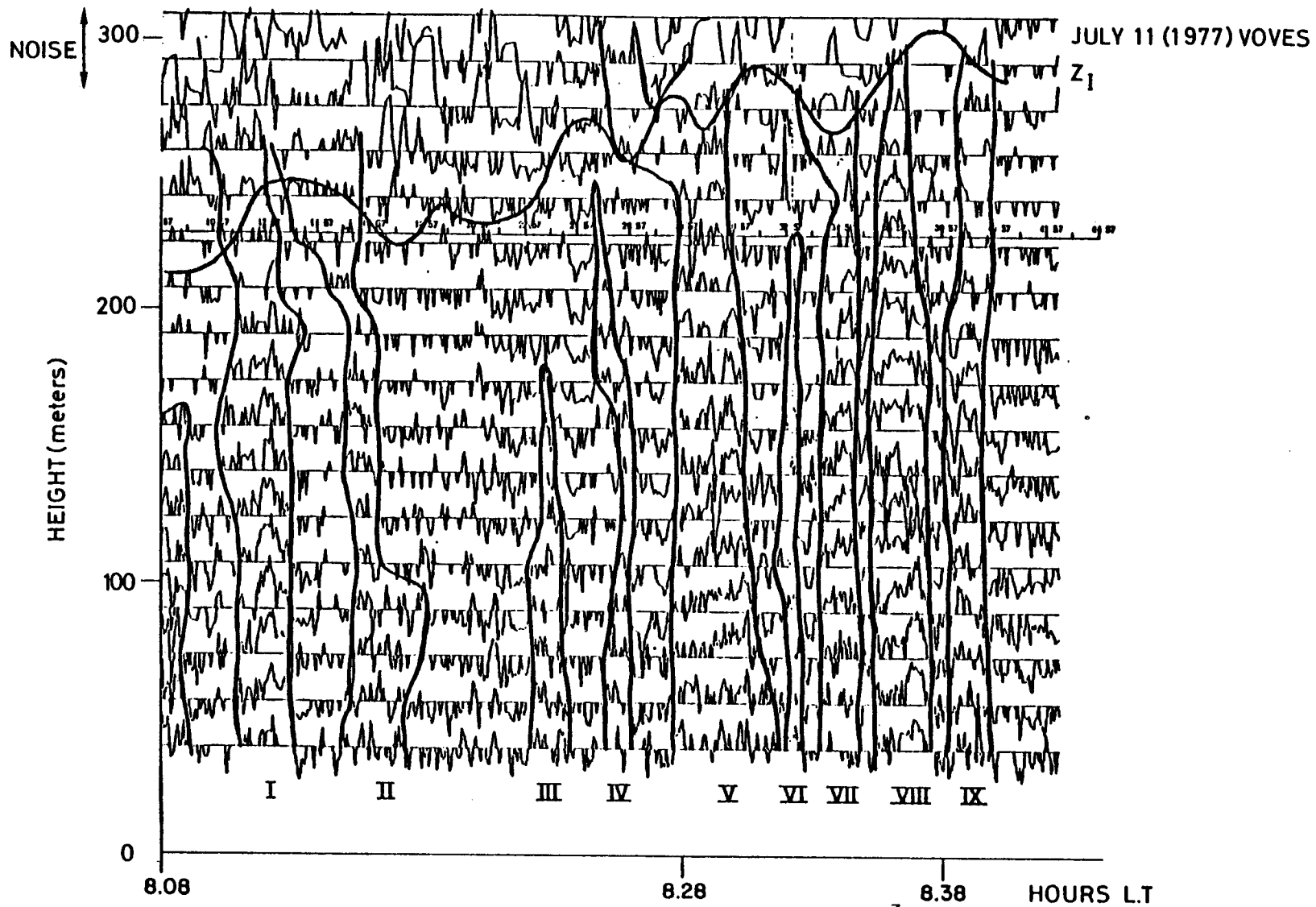
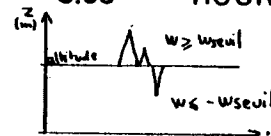
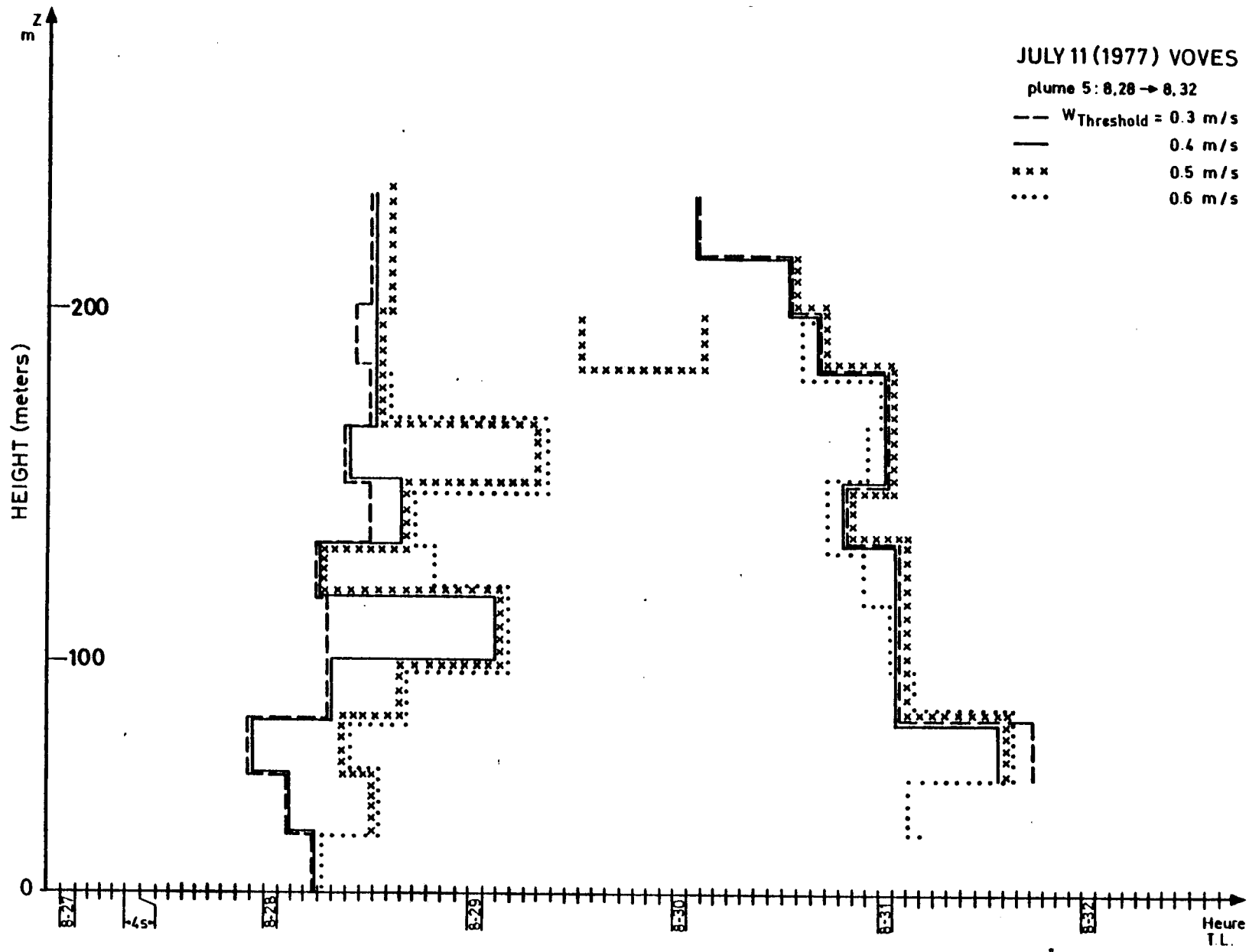


Fig. 15





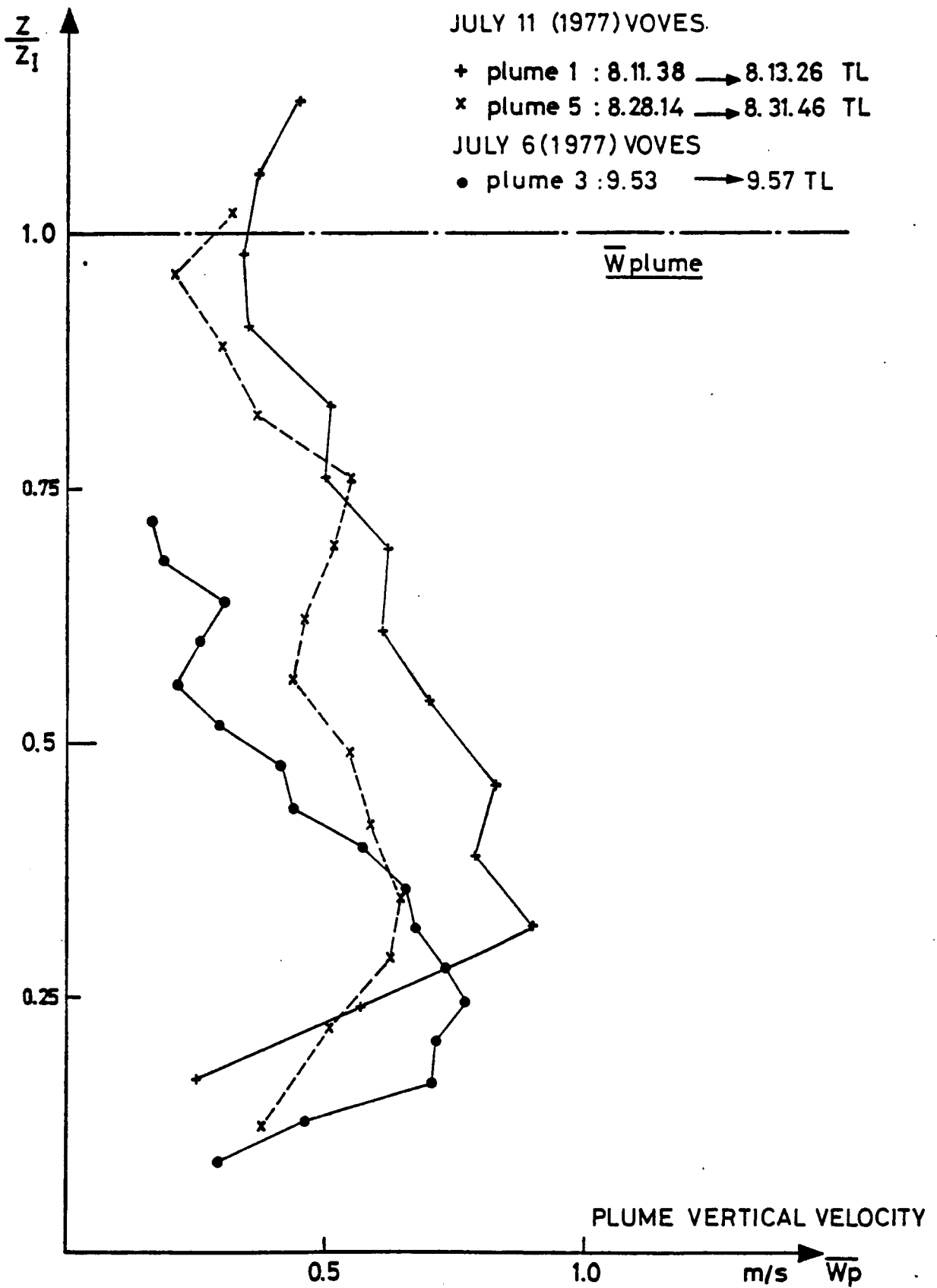


Fig.17

JULY 11 (1977) VOVES

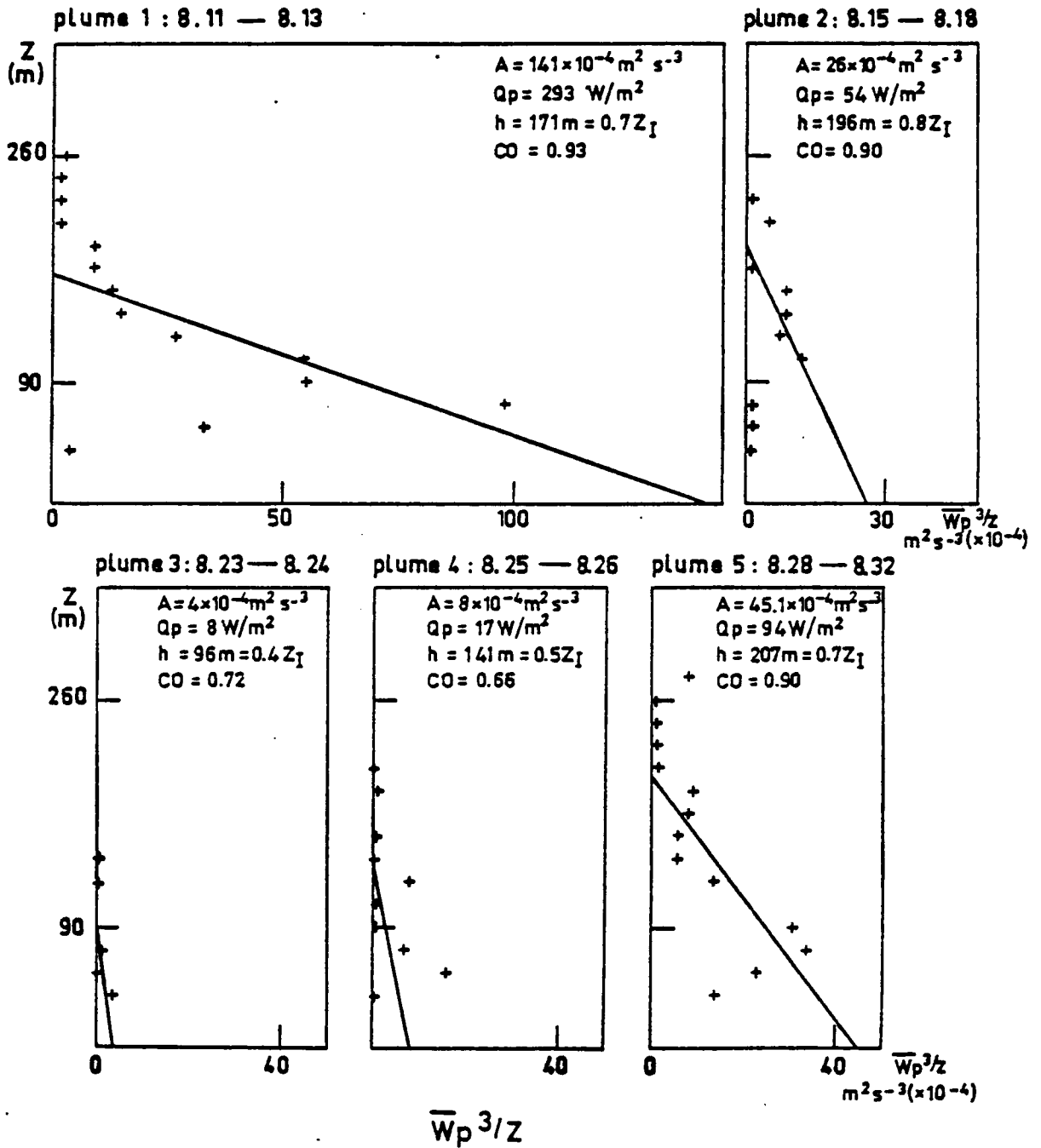
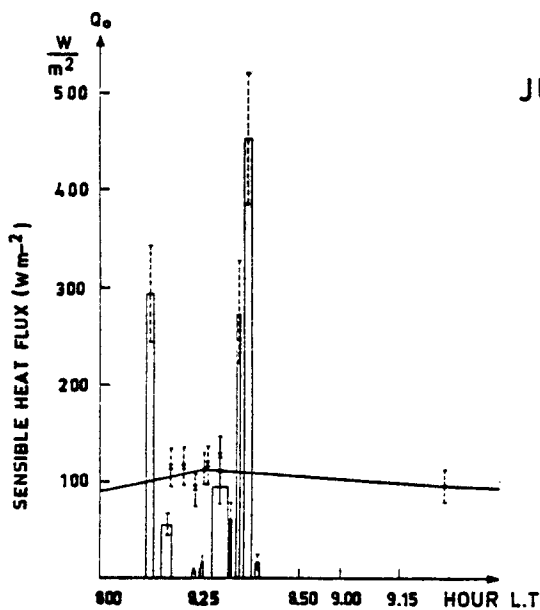
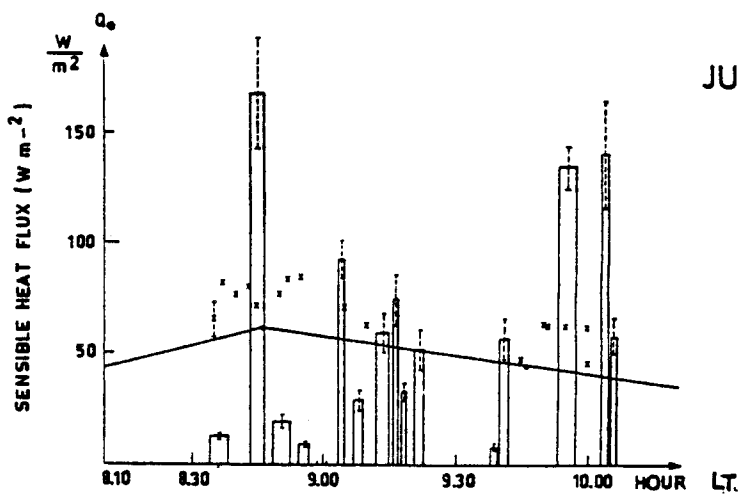
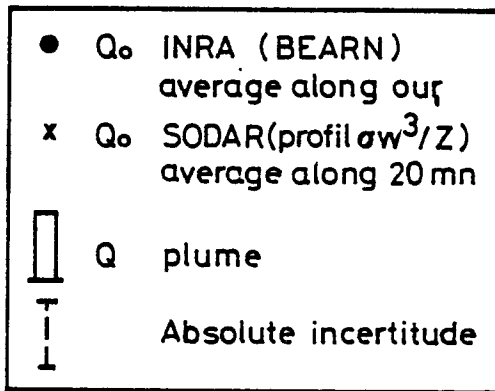


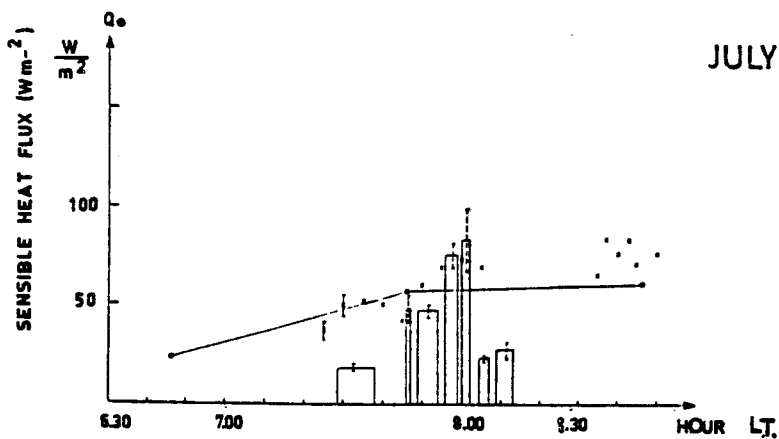
Fig. 18



JULY 11 (1977) VOVES



JULY 6 (1977) VOVES



JULY 6 (1977) VOVES

Fig. 19

JULY 6 (1977) VOVES

JULY 11 (1977) VOVES

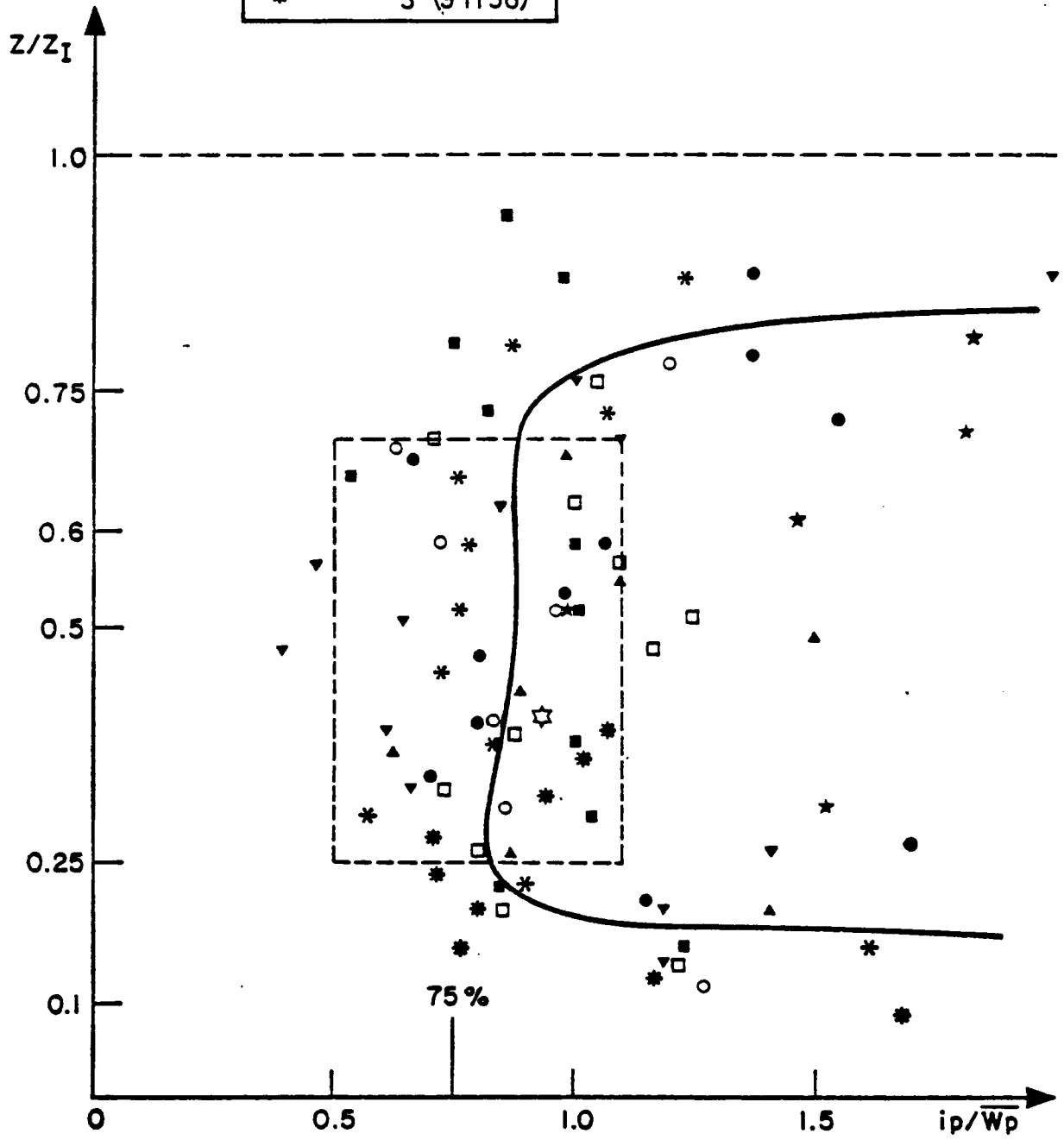
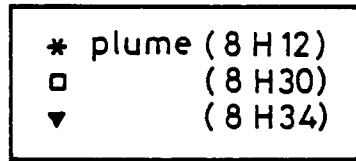
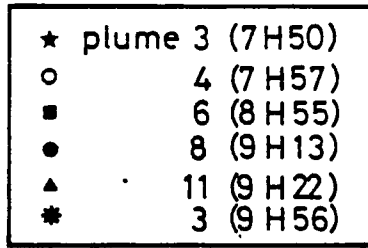


FIG. 20

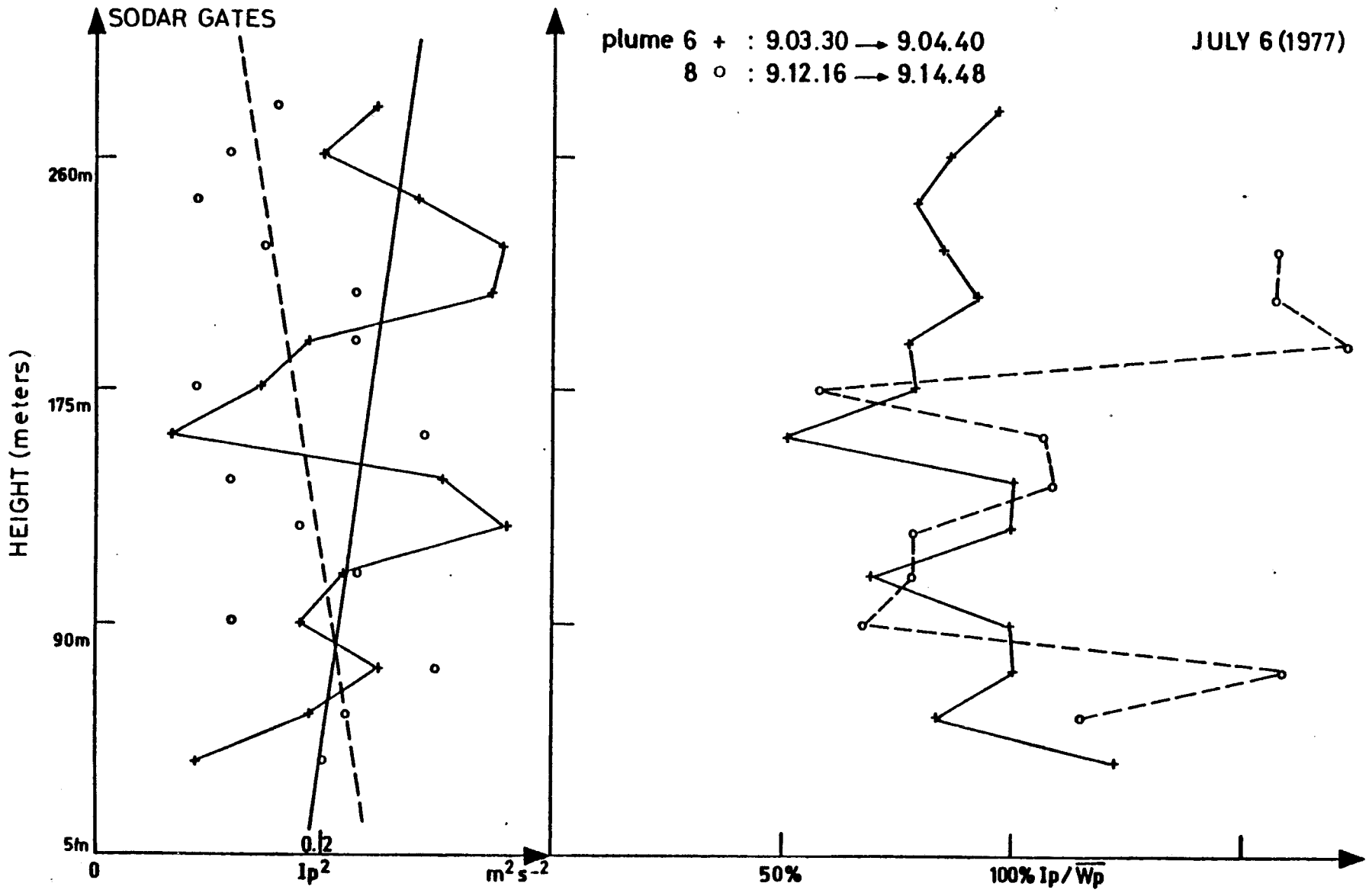


FIG. 21

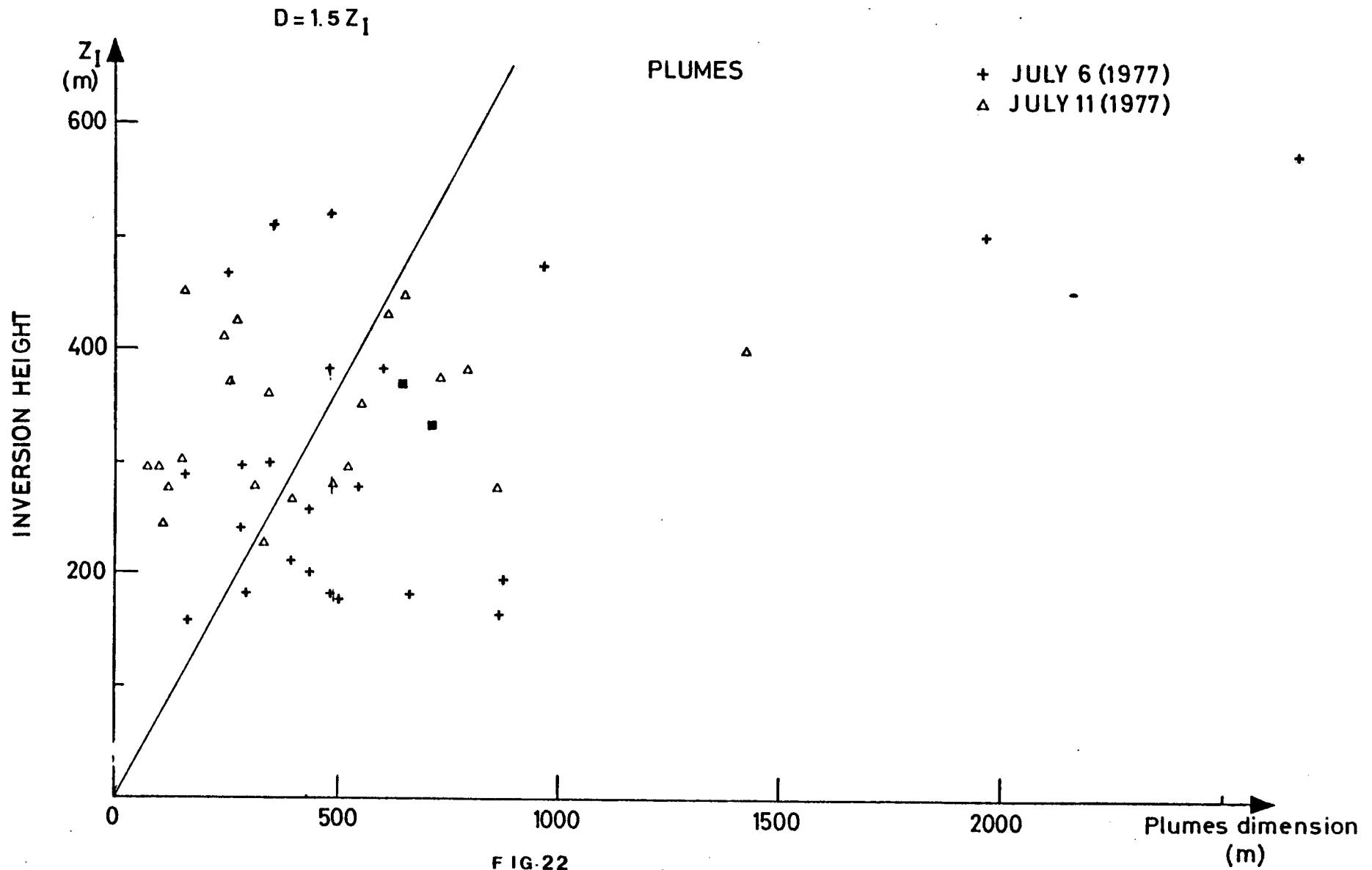


FIG-22

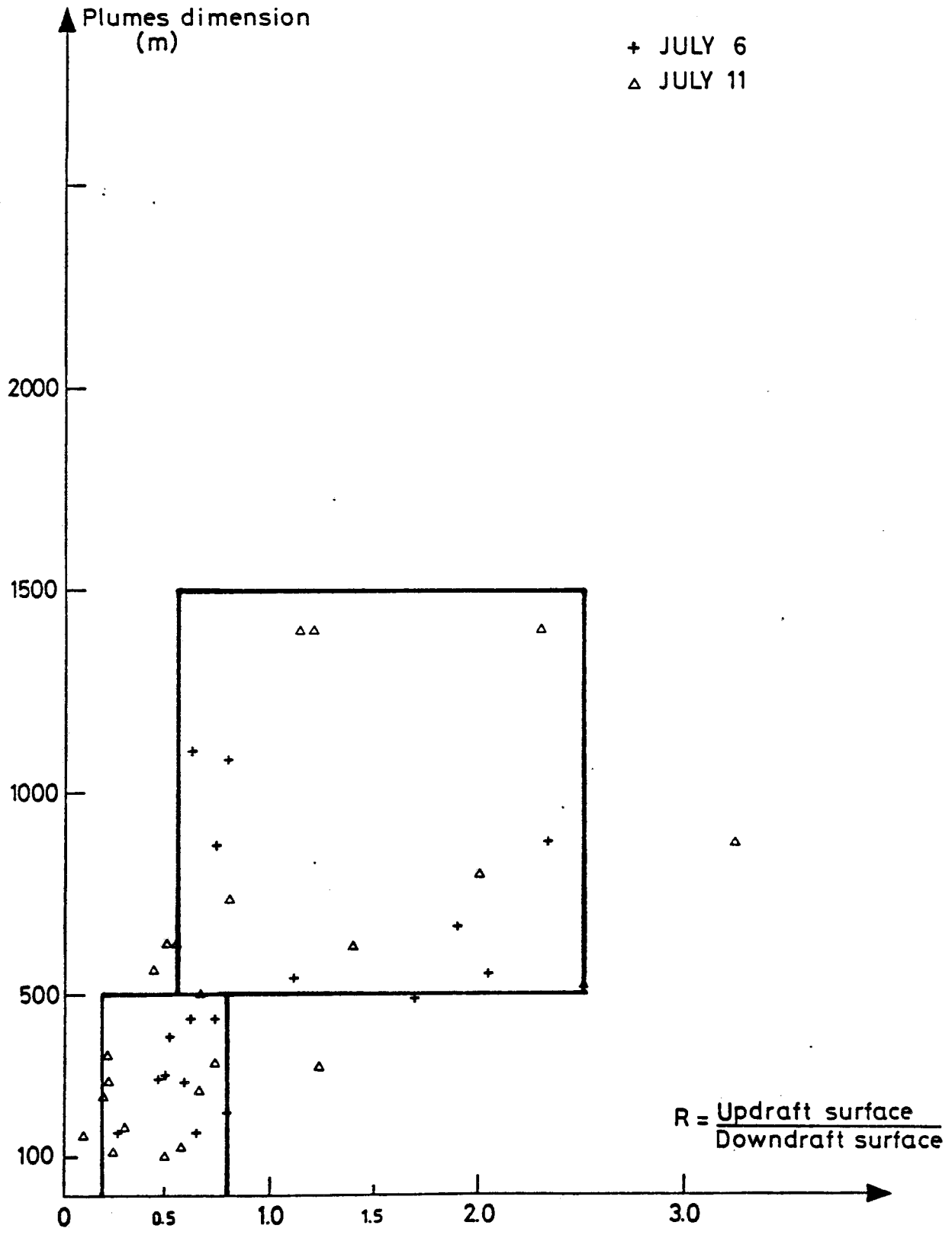
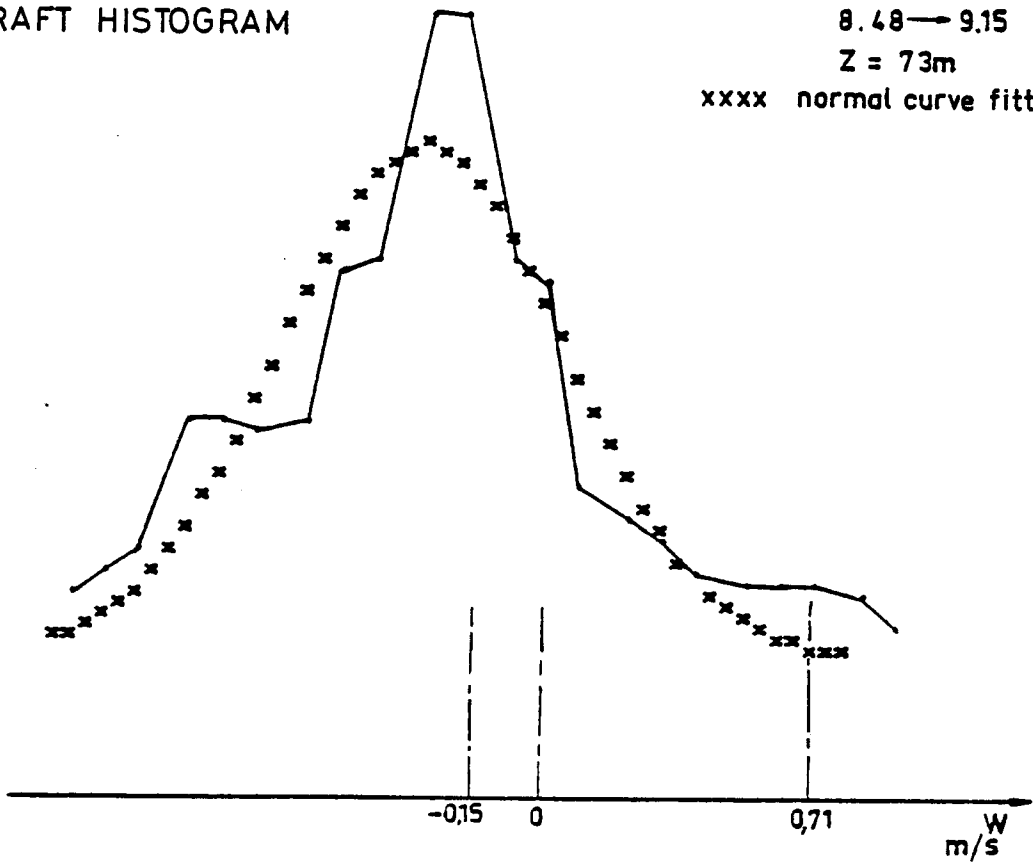


FIG. 23

DOWNDRAFT HISTOGRAM

JULY 6 (1977) VOVES
8.48 → 9.15
Z = 73m
xxxx normal curve fitting



UPDRAFT HISTOGRAM

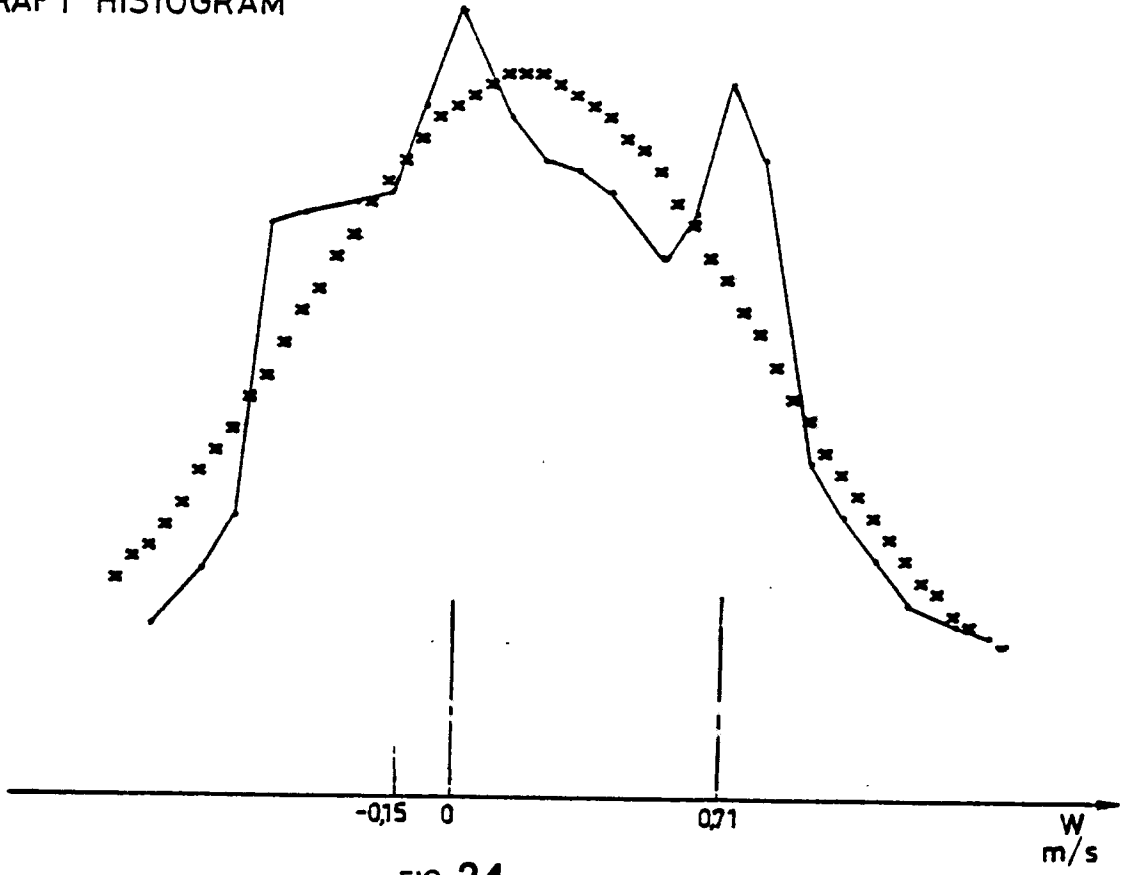


FIG. 24

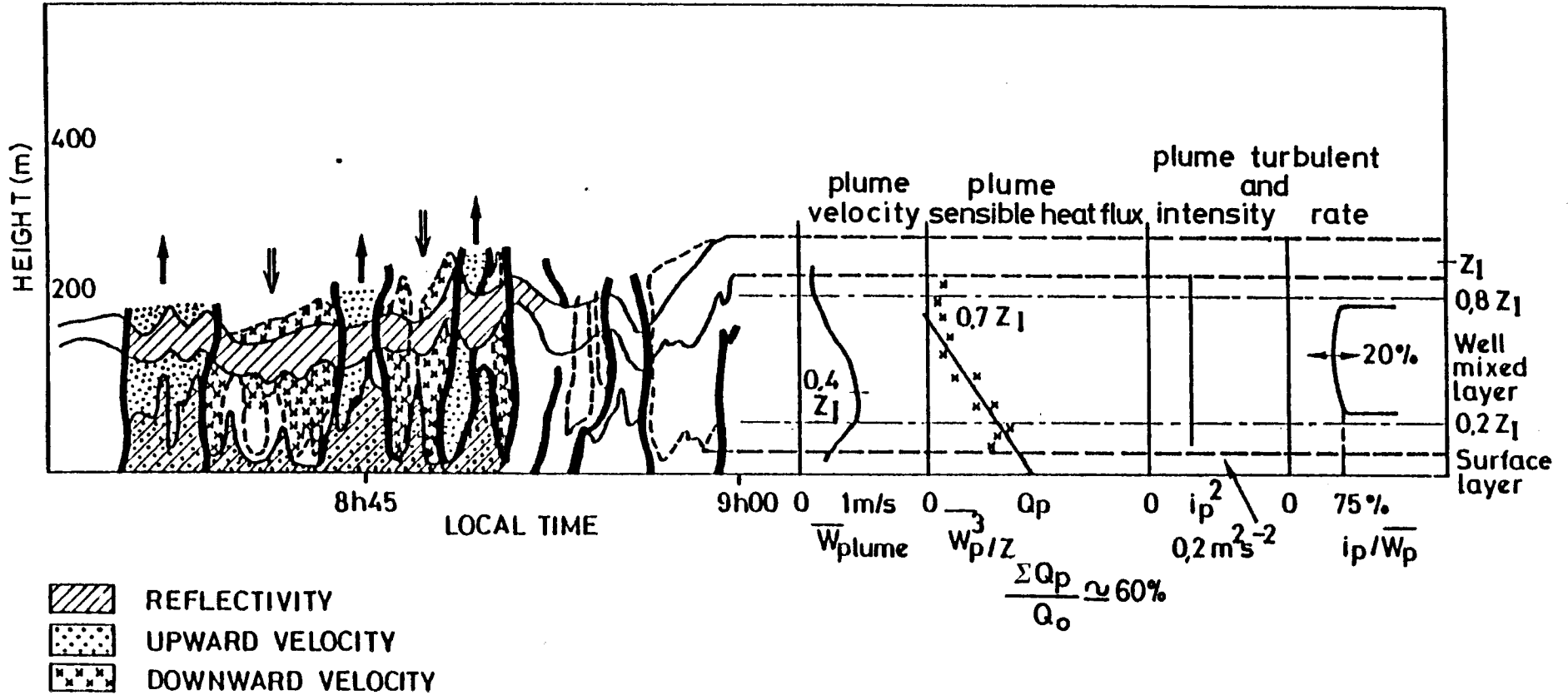


Fig. 25

CRPE
*Centre de Recherches
en Physique de l'Environnement
terrestre et planétaire*

*Avenue de la Recherche scientifique
45045 ORLEANS CEDEX*

Département PCE
*Physique et Chimie
de l'Environnement*

*Avenue de la Recherche scientifique
45045 ORLEANS CEDEX*

Département ETE
*Etudes par Télédétection
de l'Environnement*

*CNET - 38-40 rue du général Leclerc
92131 ISSY-LES-MOULINEAUX*